iScience

CellPress
OPEN ACCESS

Article

WIP1 is a novel specific target for growth hormone action

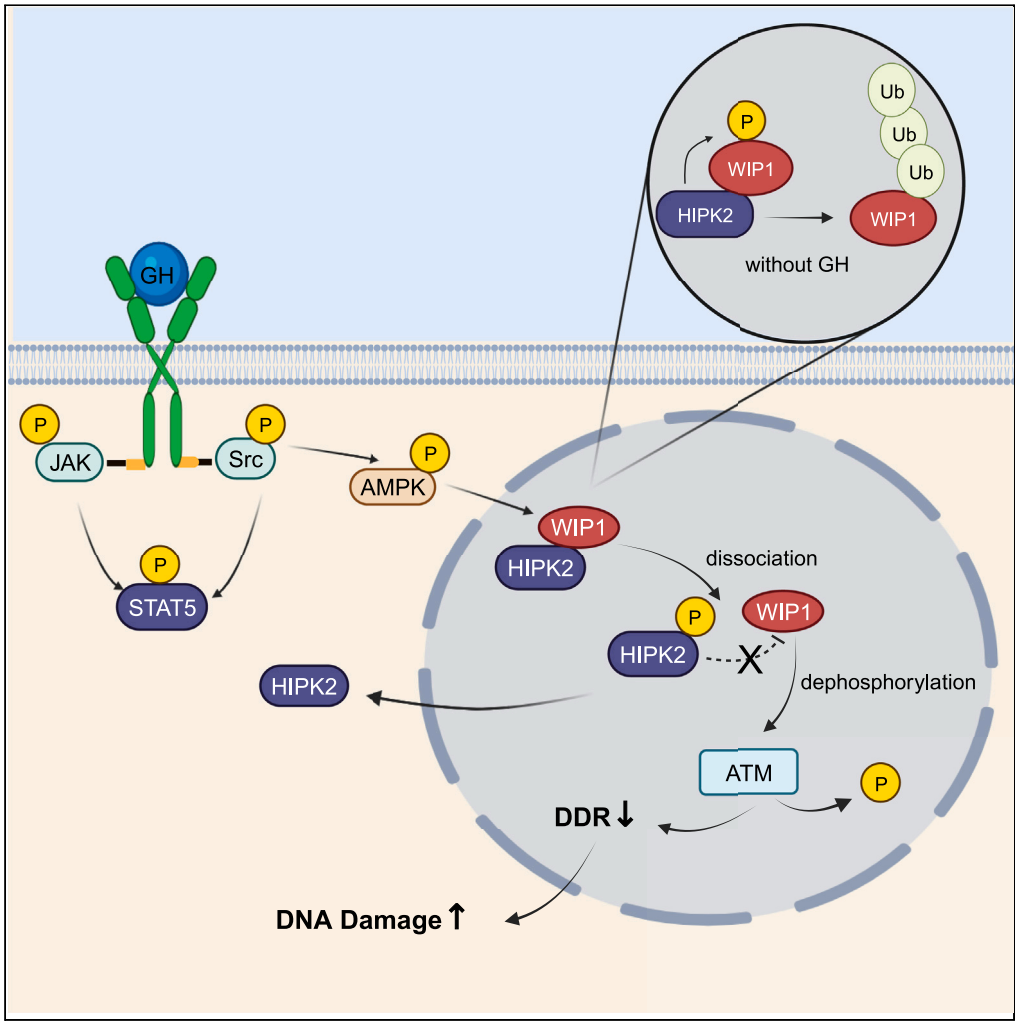

Tugce Apaydin, Svetlana Zonis, Cuiqi Zhou, ..., Jan A. Mol, Vera Chesnokova, Shlomo Melmed

melmed@csmc.edu

Highlights

Phosphatase WIP1 is a newly described target for epithelial GH action

GH suppresses DNA damage response pathway by inducing WIP1

GH acts through Src/AMPK/HIPK2, enhancing WIP1 stability

GH/WIP1 action results in unrepaired DNA damage accumulation

Apaydin et al., iScience 26, 108117
November 17, 2023
https://doi.org/10.1016/j.isci.2023.108117

iScience

CellPress
OPEN ACCESS

Article

WIP1 is a novel specific target for growth hormone action

Tugce Apaydin,[1] Svetlana Zonis,[1] Cuiqi Zhou,[1] Christian Wong Valencia,[2] Robert Barrett,[2] Ger J. Strous,[3] Jan A. Mol,[4] Vera Chesnokova,[1,5,6] and Shlomo Melmed[1,5,6,7,*]

SUMMARY

DNA damage repair (DDR) is mediated by phosphorylating effectors ATM kinase, CHK2, p53, and γH2AX. We showed earlier that GH suppresses DDR by suppressing pATM, resulting in DNA damage accumulation. Here, we show GH acting through GH receptor (GHR) inducing wild-type p53-inducible phosphatase 1 (WIP1), which dephosphorylated ATM and its effectors in normal human colon cells and three-dimensional human intestinal organoids. Mice bearing GH-secreting xenografts exhibited induced colon WIP1 with suppressed pATM and γH2AX. WIP1 was also induced in buffy coats derived from patients with elevated GH from somatotroph adenomas. In contrast, decreased colon WIP1 was observed in *GHR*$^{-/-}$ mice. WIP1 inhibition restored ATM phosphorylation and reversed GH-induced DNA damage. We elucidated a novel GH signaling pathway activating Src/AMPK to trigger HIPK2 nuclear-cytoplasmic relocation and suppressing WIP1 ubiquitination. Concordantly, blocking either AMPK or Src abolished GH-induced WIP1. We identify WIP1 as a specific target for GH-mediated epithelial DNA damage accumulation.

INTRODUCTION

DNA damage response (DDR) pathways protect the genome from DNA damage generated spontaneously during DNA replication or by exogenous agents, blocking cell-cycle progression and activating DNA repair mechanisms.[1,2] The Ser/Thr protein kinase ataxia telangiectasia mutated (ATM) kinase, key for repair of double-strand DNA breaks (DSBs),[3] is activated in response to DNA damage by Ser1981 autophosphorylation. Phospho-ATM phosphorylates DDR effectors including CHK2, p53, and H2AX (γH2AX) to ensure DNA repair and to slow damaged cell proliferation.[4–7] Abrogated DDR results in DNA damage accumulation, leading to age-associated pathological changes, tissue fragility, and neoplasia.[8,9]

Growth hormone (GH), secreted in a pulsatile fashion from the anterior pituitary, is also synthesized and secreted locally in non-pituitary tissues.[10,11] Most skeletal somatic-growth-promoting GH actions are mediated by hepatic-derived insulin-like growth factor 1 (IGF1), and GH also acts independent of IGF1 to regulate protein synthesis and metabolism.[10,12] Both endocrine and paracrine GH binds the dimeric GH receptor (GHR) to signal through the JAK/STAT pathway eliciting nuclear responses.[13,14] GH induces cell proliferation,[15,16] promotes epithelial-mesenchymal transition,[15–19] and suppresses DDR, leading to accumulated DNA damage, thus enabling a pre-neoplastic microenvironment.[16,17,20–22] GH and IGF1 have been implicated in breast, prostate, and colon neoplastic development.[21,23,24] Thus, acromegaly patients with excess GH secretion from a pituitary adenoma exhibit increased soft tissue tumors, colon polyps, and possibly adenocarcinomas[25–27]; by contrast, inherited GH signaling deficiency impedes development of malignancy in humans with Laron syndrome and also in GH-signaling-deficient mice.[28–36] We have previously shown in both normal human colon cells (hNCC) and three-dimensional intestinal organoids that GH suppressed DDR by decreasing ATM kinase activity, resulting in accumulation of unrepaired damaged DNA.[20] Moreover, hNCC with GH-induced unrepaired DNA exhibit enhanced neoplastic transformation, and mice bearing human colon adenocarcinoma (HCT116) xenografts secreting GH showed increased unrepaired colon DNA damage and more metastatic lesions.[20]

Wild-type p53-inducible phosphatase 1 (WIP1), a member of the PP2C family of Ser/Thr protein phosphatases, binds and dephosphorylates proteins involved in ATM-/ATR-initiated DDR pathways, including ATM, p53, CHK1, CHK2, Mdm2, and γH2AX.[37] WIP1 inactivates ATM by directly dephosphorylating ATM at Ser1981.[38] WIP1 also induces tumorigenesis by inactivating tumor suppressor pathways and cooperating with other oncogenes and is overexpressed in human colon and mammary cancers.[37,39,40] As WIP1 attenuates ATM kinase activity,[38] we

[1]Department of Medicine, Pituitary Center, Cedars-Sinai Medical Center, Los Angeles, CA, USA
[2]Board of Governors Regenerative Medicine Institute, Cedars-Sinai Medical Center, Los Angeles, CA, USA
[3]Center for Molecular Medicine, University Medical Center Utrecht, Institute of Biomembranes, Utrecht University, Utrecht, the Netherlands
[4]Department of Clinical Sciences of Companion Animals, Utrecht University, Utrecht, the Netherlands
[5]Senior author
[6]These authors contributed equally
[7]Lead contact
*Correspondence: melmed@csmc.edu
https://doi.org/10.1016/j.isci.2023.108117

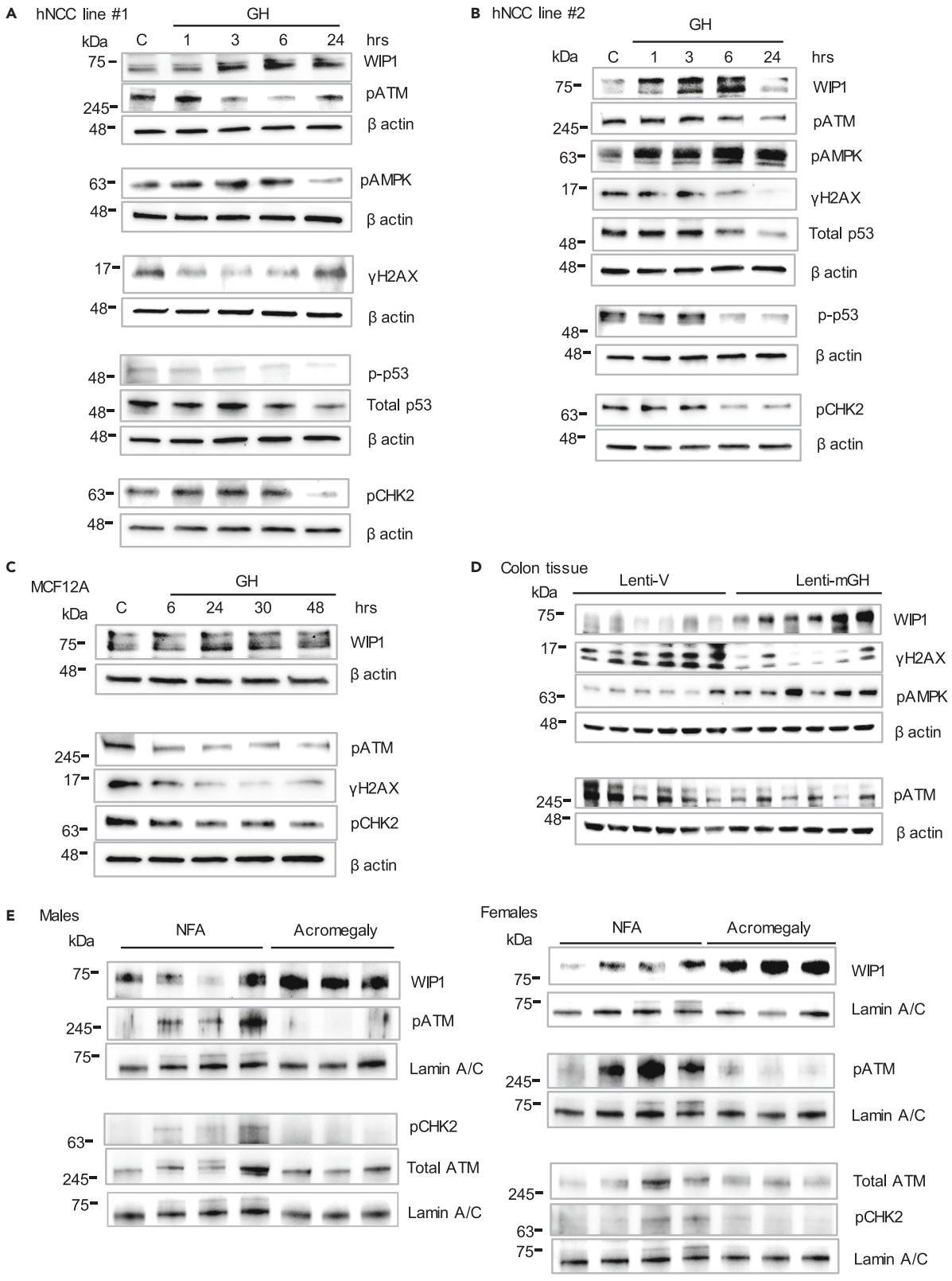
A
hNCC line #1
GH
kDa
C
1
3
6
24
hrs
75
WIP1
245
pATM
48
β actin
63
pAMPK
48
β actin
17
γH2AX
48
β actin
48
p-p53
48
Total p53
48
β actin
63
pCHK2
48
β actin
B
hNCC line #2
GH
kDa
C
1
3
6
24
hrs
75
WIP1
245
pATM
63
pAMPK
17
γH2AX
48
Total p53
48
β actin
48
p-p53
48
β actin
63
pCHK2
48
β actin
C
MCF12A
GH
kDa
C
6
24
30
48
hrs
75
WIP1
48
β actin
245
pATM
17
γH2AX
63
pCHK2
48
β actin
D
Colon tissue
Lenti-V
Lenti-mGH
kDa
75
WIP1
17
γH2AX
63
pAMPK
48
β actin
245
pATM
48
β actin
E
Males
NFA
Acromegaly
kDa
75
WIP1
245
pATM
75
Lamin A/C
63
pCHK2
245
Total ATM
75
Lamin A/C
Females
NFA
Acromegaly
kDa
75
WIP1
75
Lamin A/C
245
pATM
75
Lamin A/C
245
Total ATM
63
pCHK2
75
Lamin A/C

Figure 1. GH induces WIP1

(A–C) Western blots of (A) hNCC line #1, (B) hNCC line #2, and (C) MCF12A cells treated with GH (500 ng/mL) for indicated times; C, untreated control.

(D) Colon tissue derived from male nude mice implanted with HCT116 transduced with either lentivirus expressing murine GH (Lenti-mGH) or empty vector (Lenti-V) and sacrificed 5 weeks later. Each lane represents sample analysis derived from an individual animal.

(E) Peripheral blood buffy coats derived from patients with non-functioning adenoma (NFA; n = 4) or acromegaly (n = 3). Females and males shown separately. Each blot lane represents an individual patient. Representative blots from at least 3 independent experiments are shown. ImageJ quantifications of Western blots are depicted in Figure S1.

examined whether GH induction of DNA damage accumulation mediated by suppressing phospho-ATM, and consequently attenuating DDR, is mediated by WIP1.

Here, we identify WIP1 as a specific target for GH action. We present a heretofore undescribed mechanism whereby GH induces WIP1, in turn decreasing ATM autophosphorylation in hNCC, human normal mammary cells (MCF12A), and human intestinal organoids. We also show that WIP1 is induced in buffy coats derived from patients with active acromegaly and elevated GH levels and is induced *in vivo* in the colon of mice bearing mGH-secreting tumors with high circulating GH. WIP1 induction by GH results in suppressed DDR as evidenced by decreased phosphorylation of ATM, CHK2, H2AX, and p53, with subsequent DNA damage accumulation. By contrast, WIP1 inhibition reverses GH-induced DNA damage by restoring phosphorylation of ATM and other DDR proteins.

Intranuclear homeodomain-interacting protein kinase 2 (HIPK2) binds and inactivates WIP1.[41] In elucidating mechanisms underlying the GH/WIP1 interaction, we demonstrate that GH, by inducing Src/AMPK phosphorylation, triggers HIPK2 nuclear to cytoplasmic relocation, thereby dissociating the HIPK2-WIP1 complex, suppressing WIP1 ubiquitination, and increasing WIP1 stability. These results portray a newly described pathway for GH action in which the hormone suppresses DDR, leading to accumulated epithelial DNA damage.

RESULTS

GH induces WIP1 *in vitro*

Normal human colon cells derived from 2 de-identified patients (hNCC line #1 and hNCC line #2) were treated with human recombinant GH. Western blotting of cultured cells showed that WIP1 was induced 3–6 h after treatment (1.8-fold; $p < 0.01$). Induction of WIP1, in turn, resulted in ~45% decreased ATM phosphorylation ($p < 0.01$) and also dephosphorylated other target proteins including γH2AX, phospho-p53, and phospho-CHK2 (Figures 1A and 1B; Figures S1A and S1B). We confirmed a similar effect for GH on cultured MCF12A normal human breast cells, but likely due to a slower proliferation rate, WIP1 was induced 24 h after treatment, which, in turn, also led to decreased phosphorylation of ATM, H2AX, and CHK2 (Figure 1C; Figure S1C).

Although WIP1 is a well-known p53 target gene,[42] in our experimental model, WIP1 is induced by GH independently of p53, as GH, in fact, suppresses total p53 expression (Figures 1A and 1B; Figures S1A and S1B), consistent with our previous findings that GH decreases p53 expression by ubiquitination.[17,20,43]

High GH induces colon WIP1 *in vivo*

To confirm these results *in vivo*, twelve athymic nude male mice (6/group) were injected with human colon cancer (HCT116) cells transduced with lentivirus expressing murine GH (Lenti-mGH) or empty vector (Lenti-V) as control. All mice developed xenografted tumors 5 weeks after inoculation and those with an "acromegaly-like" model bearing mGH-expressing tumors showed increased circulating serum GH levels compared with controls (49.8 ± 7.8 ng/mL in Lenti-mGH versus 1.3 ± 0.5 ng/mL in Lenti-V; $p < 0.01$). These mice also exhibited 2.5-fold higher colon WIP1 expression, 35% decrease in phospho-ATM, and ~50% reduction in γH2AX compared with controls ($p < 0.01$) (Figure 1D; Figure S1D).

WIP1 expression is induced in peripheral blood buffy coats derived from acromegaly patients

To confirm these findings in human tissue, we collected peripheral blood buffy coats derived from female and male patients with acromegaly harboring GH-secreting pituitary adenomas (3/group) and from patients with non-functioning pituitary adenomas (NFA) (4/group) and normal levels of GH. We observed a 2-fold increase in WIP1 expression in samples derived from female and male acromegaly patients with high GH levels, as compared with samples derived from NFA patients with normal GH levels. Moreover, phospho-ATM was decreased by 50% in samples derived from female and male acromegaly patients. CHK2 phosphorylation was reduced in female acromegaly patients ~35% ($p < 0.05$), but the reduction did not reach statistical significance in male patients with acromegaly (Figure 1E; Figure S1E).

GH activates WIP1 through GHR signaling

To elucidate whether induction of WIP1 occurs via GHR activation, hNCC were pretreated with 20 μg/mL pegvisomant, a GHR antagonist, for 1 h and then treated with GH for 24 h. In cells pretreated with pegvisomant, GH-induced WIP1 expression was prevented, and GH-induced suppression of ATM phosphorylation was abolished (Figure 2A; Figure S2A), suggesting GHR-mediated GH action on WIP1.

Next, we examined colon tissue derived from wild-type (WT) and $GHR^{-/-}$ male mice. Concordant with *in vitro* results shown earlier, 3-month-old $GHR^{-/-}$ mice devoid of GH signaling showed decreased colon WIP1 expression as compared with WT, and this decrease became markedly more pronounced at 24 months (Figure 2B; Figure S2B).

Together, these results indicate that GH effects on WIP1 are GHR-mediated.

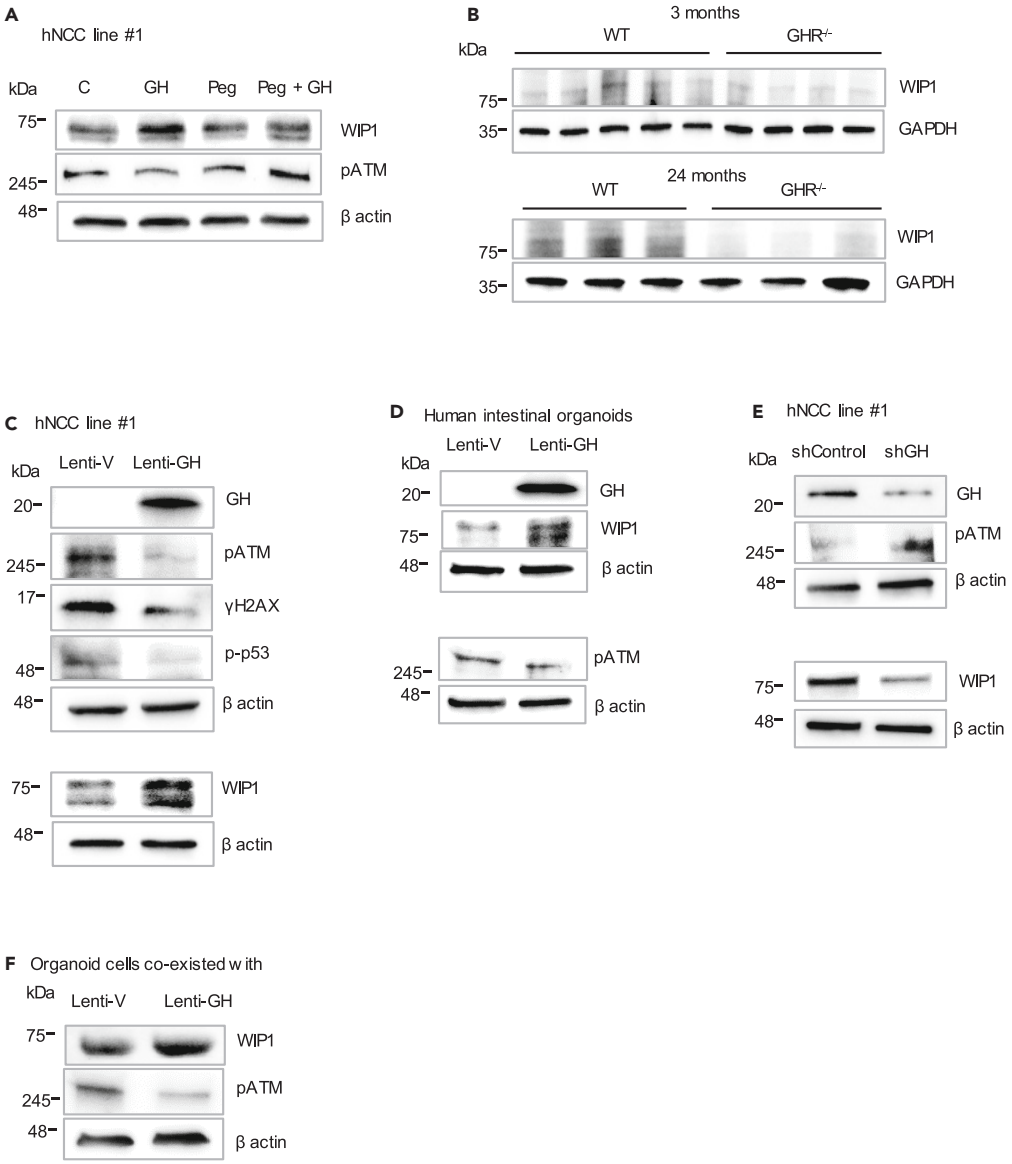

Figure 2. GH induces WIP1 through GHR signaling

(A) Western blots of hNCC line #1 pretreated with 20 mg/mL pegvisomant (Peg) for 1 h then treated with GH (500 ng/mL) for an additional 24 h. C, untreated control.

(B) Colon tissue derived from 3- and 24-month-old WT and *GHR*$^{-/-}$ male mice. Each lane represents sample analysis derived from an individual animal.

(C) hNCC line #1 transduced with lentivirus expressing GH (Lenti-GH) or empty vector (Lenti-V) and analyzed 10 days later.

(D) iPSC-derived human intestinal organoid lines from 3 different patients were transduced with Lenti-V or Lenti-GH and analyzed 5 weeks later. Representative blots from one human intestinal organoid line are shown.

(E) hNCC line #1 transduced with lentivirus expressing control shRNA (shControl) or GH shRNA (shGH).

(F) Three different human intestinal organoid lines were transduced with GFP-expressing Lenti-V or Lenti-GH and cultured for 5 weeks, then sorted for GFP-negative cells. GFP-negative cells co-existing in organoids with either Lenti-GH or Lenti-V expressing cells were analyzed. All lines exhibited similar results. Representative blots from one human intestinal organoid line are shown. Representative blots from at least 3 independent experiments are depicted. ImageJ quantifications of western blots are depicted in Figure S2.

Autocrine/paracrine GH increases WIP1 expression

As endogenous GH is induced in epithelial colon cells after acute DNA damage or in senescent cells,[11,43] we tested whether autocrine/paracrine GH affects WIP1 using hNCC and three-dimensional intestinal organoids.

To evaluate autocrine GH action, hNCC and organoid lines derived from 3 different patients were transduced with Lenti-GH or Lenti-V and analyzed after 10 days and 5 weeks, respectively. GH-expressing hNCC and all 3 organoid lines showed higher WIP1 and lower phospho-ATM

expression (Figures 2C and 2D; Figures S2C and S2D). By contrast, GH suppression with lentivirus expressing GH shRNA (shGH) in hNCC downregulated WIP1, with increased levels of phospho-ATM (Figure 2E; Figure S2E).

To assess paracrine GH effects, organoids were transduced with Lenti-V or Lenti-GH, both expressing GFP. Approximately 60% of organoid cells were positive for GFP. We tested how GH from infected cells acts on intact neighboring cells. Therefore, 5 weeks after transduction, organoids were dispersed and sorted for GFP-positive cells (expressing either Lenti-GH or Lenti-V) and GFP-negative intact neighboring cells. Only GFP-negative cells co-existing in organoids with either Lenti-GH or Lenti-V expressing cells were analyzed. GH concentration confirmed by ELISA in the Lenti-GH organoid medium was 98.8 $\pm$ 4.4 ng/mL and was undetectable in the culture medium of Lenti-V organoids ($p < 0.01$). In all 3 organoid lines, WIP1 was induced and phospho-ATM was markedly decreased in cells growing in close proximity to cells expressing and secreting GH (Figure 2F; Figure S2F).

These results support autocrine and/or paracrine GH enhancement of WIP1 phosphatase expression and attenuation of ATM phosphorylation, similar to that seen for endocrine GH action (Figure 1).

GH suppresses DDR by inducing WIP1

We next examined whether GH-mediated suppressed ATM phosphorylation could be reversed by WIP1 inhibition.[37,44] We blocked WIP1 expression using GSK2830371, a selective small molecule inhibitor of WIP1 phosphatase enzymatic activity that induces ubiquitin-mediated WIP1 degradation.[44] We pre-treated hNCC with 5 μM or 10 μM of GSK2830371 for 1 h, then added GH for 24 h. GH suppression of phospho-ATM and γH2AX were reversed when WIP1 was downregulated (Figure 3A; Figure S3A).

Experiments with intestinal organoids confirmed these results. Although treatment with GH for 48 h suppressed ATM, CHK2, and H2AX phosphorylation at baseline, blocking WIP1 expression restored DDR protein phosphorylation in GH-treated organoids ($p < 0.01$; Figure 3B; Figure S3B).

Similar results were obtained by inhibiting WIP1 using WIP1 siRNA. hNCC were nucleofected with either siScr (control) or siWIP1, and 5 h after nucleofection, media was changed and cells treated with GH for an additional 6 h. Blocking WIP1 resulted in increased pATM expression in hNCC treated with GH compared with control siScr-infected cells ($p < 0.01$, Figure S3C and S3D).

To assess DNA damage after inhibition of WIP1, we performed single-cell gel electrophoresis (Comet assay) in hNCC treated with WIP1 inhibitor with or without GH for 24 h. DNA damage was increased ~60% in cells treated with GH only, whereas blocking WIP1 in these cells restored accumulated DNA damage to control levels ($p < 0.01$) (Figure 3C).

These results are consistent with the notion that GH suppression of DDR is mediated by induced WIP1.

GH decreases WIP1 ubiquitination

Next, we assessed mechanisms underlying WIP1 upregulation by GH. As WIP1 mRNA expression did not change in response to GH treatment (Figure S4A), we considered whether the GH effect was due to WIP1 protein ubiquitination. Accordingly, hNCC were treated with GH for 24 h and protein lysates immunoprecipitated with IgG or anti-ubiquitin antibodies. Immunoblotting revealed that GH treatment decreased WIP1 binding to ubiquitin (Ub) (Figure 4A; Figure S4B).

Degradation of WIP1 by ubiquitination is mediated by binding to HIPK2,[41] which itself is induced in response to DNA damage.[45] Therefore, to induce both HIPK2 and WIP1, we treated hNCC with 20 μM of DNA-damage-inducing etoposide for 24 h, and, after washing, treated the cells with GH for an additional 24 h. As expected, HIPK2, WIP1, and Ub were all induced by etoposide (2.2-, 1.8-, and 3.3-fold, respectively; $p < 0.01$), and WIP1 and Ub were further induced after GH treatment (3-, 2.2-, and 5.8-fold, respectively; $p < 0.01$) (Figure 4B; Figure S4C). Immunoprecipitation with Ub antibodies after etoposide treatment showed that although etoposide-induced total Ub expression was higher in the presence of GH, binding of WIP1 to Ub was decreased by GH (Figure 4C; Figure S4D).

To assess whether effects of GH on WIP1 are mediated through HIPK2, we performed immunoprecipitation using anti-HIPK2 antibodies. When hNCC were treated with etoposide and GH as discussed earlier, GH decreased WIP1 binding to HIPK2, indicating less HIPK2-mediated WIP1 degradation in the presence of GH (Figure 4D; Figure S4E). We also confirmed these results in cell lysates immunoprecipitated with anti-WIP1 antibodies, demonstrating decreased binding of WIP1 to HIPK2 and of WIP1 ubiquitination in GH-treated cell lysates (Figure 4E; Figure S4F).

GH induces nuclear-cytoplasmic HIPK2 translocation

As total HIPK2 protein expression did not change after GH treatment (Figure 4B; Figure S4C), we considered whether GH alters HIPK2 localization. We therefore isolated cytoplasmic and nuclear protein fractions from hNCC after 6 and 24 h of GH treatment, respectively. GH caused a 50% decline in nuclear fraction HIPK2 abundance, whereas cytoplasmic HIPK2 expression was increased ~60% (Figure 4F; Figure S4G), indicating that GH triggers HIPK2 cytoplasmic relocation. WIP1 is mainly localized in the nucleus[37,42] and GH decreased HIPK2 in the nuclear fraction, resulting in further increased nuclear WIP1 and reduced ATM phosphorylation (Figure 4F; Figure S4G), suggesting that GH induces WIP1 by enabling nuclear to cytoplasmic HIPK2 translocation, thus diminishing HIPK2 binding to and inactivation of intranuclear WIP1.

These observations were supported by immunocytochemistry showing low basal WIP1 nuclear expression and abundant nuclear HIPK2 localization (Figure 4G), concordant with previous findings.[42,46] GH treatment markedly diminished nuclear HIPK2 expression while increasing nuclear WIP1 expression (Figure 4G). These results supported the conclusion that GH stabilizes WIP1 by enabling HIPK2 translocation from the nucleus.

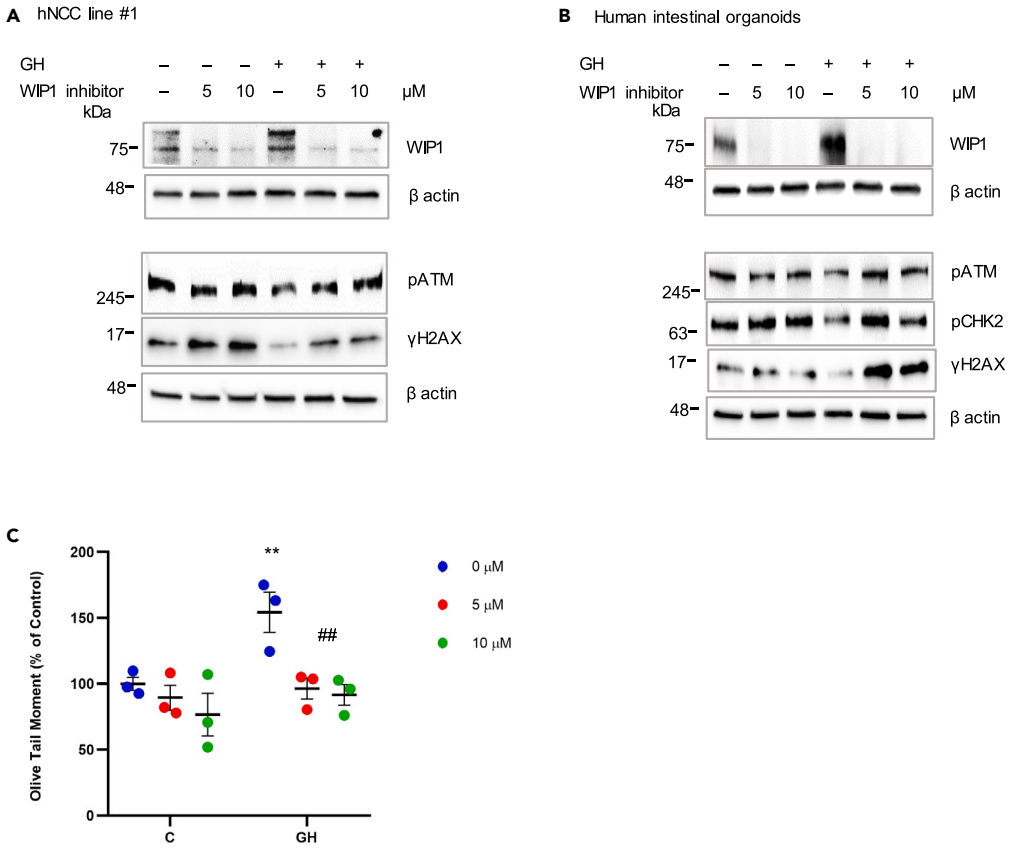

Figure 3. Blocking WIP1 increases DDR protein phosphorylation and decreases unrepaired DNA damage

(A and B) Western blots of (A) hNCC line #1 treated with WIP1 inhibitor (GSK2830371) for 1 h followed by GH (500 ng/mL) for an additional 24 h and (B) organoids treated with WIP1 inhibitor and GH (500 ng/mL) for 48 h. Untreated cells served as control. Representative blots from at least 3 independent experiments are shown. ImageJ quantification of western blots is depicted in Figure S3.

(C) Comet assay of hNCC line #1 treated with WIP1 inhibitor for 1 h followed by GH (500 ng/mL) for an additional 24 h. C, control. Single-cell gel electrophoresis was conducted and Olive tail moment assessed on at least 400 cells/per slide for each experiment. Results are shown as mean of 3 experiments ±SEM. Differences were assessed with non-parametric Kruskal-Wallis test followed by Dunn's multiple comparison test. **$p < 0.01$ versus control; ##$p < 0.01$ GH versus GH + WIP1 inhibitor.

GH-induced WIP1 upregulation is mediated by phospho-AMPK

We further examined mechanisms mediating GH effects on HIPK2/WIP1. AMPK, a Ser/Thr protein kinase, phosphorylates HIPK2 and suppresses WIP1 degradation by dissociating WIP1 from HIPK2.[41] In both hNCC lines, we observed 1.5-fold increased phospho-AMPK expression for 1 to 6 h after GH treatment ($p < 0.01$) (Figures 1A and 1B; Figures S1A and S1B), and mice bearing mGH-secreting tumors also exhibited higher levels of colon phospho-AMPK (Figure 1D; Figure S1D) concordant with WIP1 induction. Furthermore, blocking AMPK kinase activity in hNCC with permeable Compound C, a pyrazolopyrimidine,[46] decreased GH-associated WIP1 induction (Figure 5A; Figure S5A). These results were reproduced in intestinal organoids, where blocking AMPK phosphorylation led to reduced WIP1 induction by GH (Figure 5B; Figure S5B).

GH induces WIP1 expression via Src/AMPK/HIPK2 pathway

Src activation leads to HIPK2 phosphorylation at Tyr354 and its subsequent inactivation and cytoplasmic relocation.[45,47] As Src activates AMPK,[48–50] and as GH binding to GHR results in Src autophosphorylation,[13,51] we examined whether GH effects on AMPK/HIPK2/WIP1 are mediated by Src. In hNCC treated with GH, Src phosphorylation increased 2-fold at 30 min ($p < 0.01$) and 1.3-fold at 60 min after treatment ($p < 0.05$) (Figure 5C; Figure S5C). Blocking Src phosphorylation by the tyrosine kinase inhibitor dasatinib (Figure 5D; Figure S5D) abolished WIP1 induction by GH (Figure 5E; Figure S5E). To test whether Src regulates AMPK activity, hNCC were treated with Src inhibitor for 24 h and then with GH for 3 h. Treatment with the Src inhibitor reversed GH-related increased AMPK phosphorylation (Figure 5F; Figure S5F).

To confirm the specificity of these results, hNCC were transduced with lentivirus expressing Src shRNA (shSrc) or control shRNA (shControl) and analyzed 72 h after transduction (Figure 5G; Figure S5G). Although treatment with GH for 3 h resulted in increased AMPK phosphorylation in shControl transfectants, there was no up-regulation in hNCC where Src was suppressed (Figure 5H; Figure S5H). However, we also

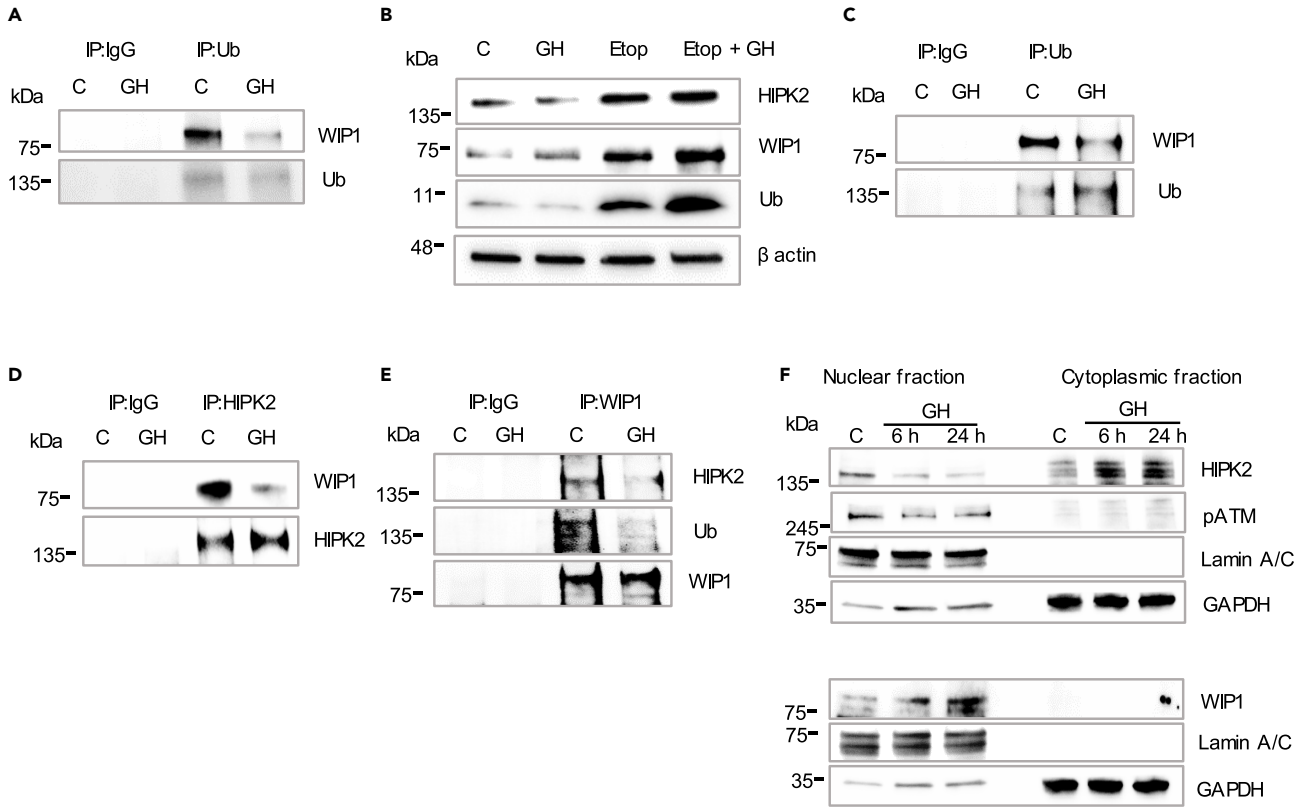

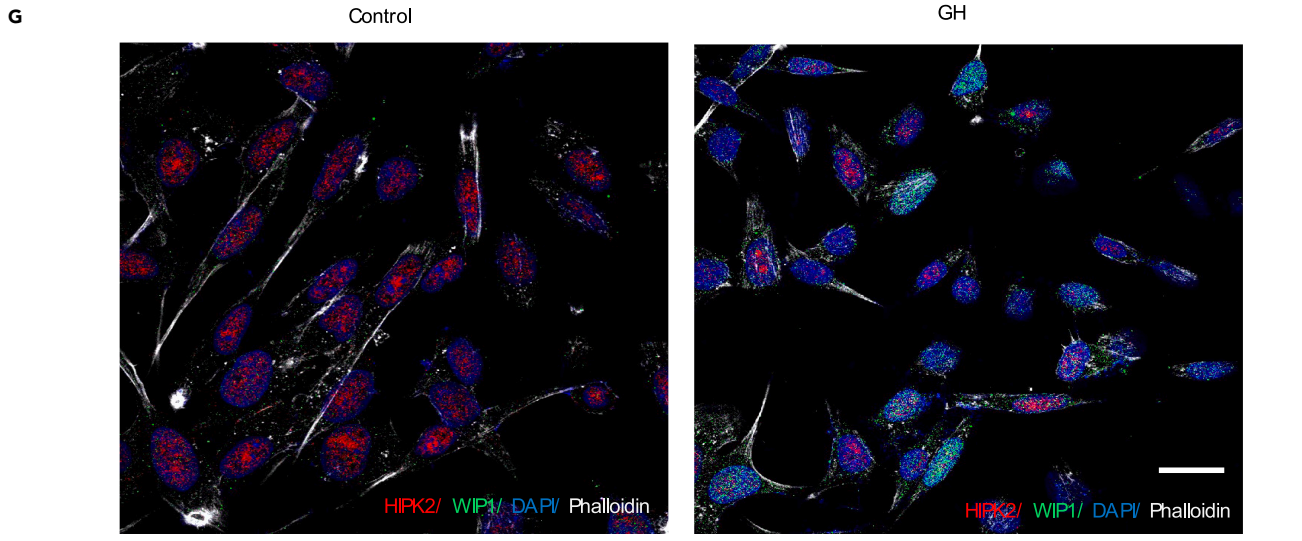

Figure 4. GH triggers HIPK2 cytoplasmic relocation and induces nuclear WIP1 stability by reducing ubiquitination

(A) hNCC line #1 was treated with GH (500 ng/mL) for 24 h, and cell lysates were immunoprecipitated (IP) with IgG or anti-ubiquitin (Ub) antibodies and immunoblotted for WIP1. C, control.

(B) Western blot of whole-cell lysates. hNCC line #1 was treated with 20 μM etoposide for 24 h, then with GH (500 ng/mL) after washout for an additional 24 h.

(C) WIP1 and ubiquitin (Ub) interactions were analyzed in hNCC line #1 treated with 20 μM etoposide for 24 h, then with GH (500 ng/mL) after washout for an additional 24 h. Cell lysates were immunoprecipitated with IgG or anti-ubiquitin antibodies and immunoblotted for WIP1 and Ub.

(D) WIP1 and HIPK2 interactions analyzed in hNCC line #1 treated with 20 μM etoposide for 24 h, then with GH (500 ng/mL) after washout for an additional 24 h. Cell lysates were immunoprecipitated with IgG or anti-HIPK2 antibodies and immunoblotted for WIP1 and HIPK2.

Figure 4. *Continued*

(E) WIP1, HIPK2, and Ub interactions analyzed in hNCC line #1 treated with 20 μM etoposide for 24 h, then with GH (500 ng/mL) after washout for additional 24 h. Cell lysates were immunoprecipitated with IgG or anti-WIP1 antibodies and immunoblotted for anti-HIPK2, Ub, and WIP1.

(F) Western blots of cytoplasmic and nuclear fractions of expressed proteins in hNCC line #1 left untreated (C) or treated with GH (500 ng/mL) for 6 h and 24 h. ImageJ quantifications of western blots are depicted in Figure S4.

(G) Confocal images of hNCC line #1 untreated (Control) or treated with GH (500 ng/mL) for 24 h and stained for HIPK2 (red), WIP1 (green), DAPI (blue), and phalloidin (white). Scale bar, 20 μm.

observed that GH decreased phospho-AMPK in cells expressing shSrc, which we cannot yet explain, and may reflect other pathways activated with blocking Src.

When Src was suppressed in hNCC, GH failed to induce WIP1 and suppress phospho-ATM (Figure 5I; Figure S5I).

Blocking GH signaling with BM001, a small molecule that inhibits GHR synthesis[52] (Figure 6A; Figure S6A), also inhibited Src/AMPK phosphorylation (Figures 6B and 6C; Figures S6B and S6C), subsequently inhibiting WIP1 and activating ATM phosphorylation (Figure 6D; Figure S6D).

To confirm these results *in vivo*, eight 3-month-old female mice (4/group) were injected i.p. with DMSO or BM001 (3 mg/kg) 3 times/week for 3 weeks. BM001-treated mice exhibited lower colon GHR and WIP1 expression, whereas phospho-ATM was upregulated in these animals (Figure 6E; Figure S6E).

Overall, the results suggest that GH-induced Src/AMPK/HIPK2/WIP1 signaling cascade leads to accumulated DNA damage in epithelial cells.

DISCUSSION

Our results identify the WIP1 phosphatase as a target for GH action. We previously showed that GH attenuated DDR pathway by suppressing ATM kinase activity.[20] Here, we demonstrate that GH reduces DDR activation by inducing WIP1, which subsequently dephosphorylates ATM and its downstream targets, including p53, CHK2, and H2AX. We also elucidate mechanisms underlying stimulatory effects of GH on WIP1.

DDR protects the cell against genomic instability and constrains proliferation of DNA-damaged cells.[53] DNA damage leads to ATM autophosphorylation, which, in turn, phosphorylates CHK2 to arrest DNA-damaged cell proliferation, phosphorylates H2AX to mark sites of DNA damage, and phosphorylates and stabilizes p53 to enable DNA repair.[4,54] Inadequate DDR may result in accumulated DNA damage with subsequent cellular transformation[55] and inactivation of cell-cycle checkpoint proteins, including ATM, CHK2, and ATR kinase, required for progression of pre-malignant tumors.[54,56,57]

The amplified *PPM1D* gene encoding WIP1 and overexpressed WIP1 protein occur in colorectal cancer, where WIP1 expression correlated with stage and metastasis.[40] WIP1 limits DDR activity by suppressing ATM phosphorylation,[37] thus leading to further tumor growth.[38] Consistent with these observations, mice lacking WIP1 exhibited higher levels of phospho-ATM[38] and were resistant to tumorigenesis.[58] Removing WIP1 from a tumor-prone ATM-null mouse reduced tumorigenesis and decreased genomic instability.[59]

We had reported that DNA damage triggers GH expression, which, in turn, reduces ATM phosphorylation and, by suppressing ATM kinase activity, destabilizes p53, thus enhancing colon cell neoplastic transformation.[17,20] Moreover, we observed that GH-related suppression of colon DNA damage response occurs independent of IGF1.[12] We show here that GH alters DDR activity by inducing WIP1, which dephosphorylates ATM, CHK2, p53, and H2AX, resulting in accumulated unrepaired DNA damage. These results were confirmed *ex vivo* when we observed increased WIP1 expression in peripheral blood buffy coats derived from patients with acromegaly, as well as in the colon of mice bearing GH-secreting xenografts and showing lower phospho-ATM and γH2AX levels. Conversely, blocking GH signaling with the GHR antagonist pegvisomant or the GHR synthesis inhibitor BM001, or blocking endogenous GH expression with shGH RNA in hNCC, decreased expression of WIP1 and restored ATM phosphorylation, concordant with our observation of decreased colon WIP1 expression in $GHR^{-/-}$ mice devoid of GH signaling. These results elucidate mechanisms underlying our previously published observation of increased unrepaired DNA damage in the colon of GH-secreting xenograft-bearing mice versus decreased DNA damage in aging $GHR^{-/-}$ mice.[43] These mechanisms may also underpin pro-tumorigenic GH properties described in human cancers,[23,60,61] acromegaly patients,[25,27,62] and GH transgenic mice that exhibit increased rates of mammary tumors and hepatocellular cancer.[62–65] Our results also explain why GH signaling deficiency protects Laron syndrome patients from developing cancers[34,35] and why disruption of GHR in experimental models leads to reduced incidence of colon, mammary, and prostate tumors.[30,62]

WIP1 is maintained at low baseline levels[41,42] by binding to and being inactivated by the nuclear serine/threonine kinase HIPK2.[41] WIP1 is phosphorylated by HIPK2, and phosphorylated WIP1 undergoes polyubiquitination followed by proteasomal degradation, whereas HIPK2 depletion stabilizes WIP1.[41] Impaired HIPK2 activity also occurs in colorectal and breast cancers.[66,67] In elucidating mechanisms for GH-associated WIP1 induction, we observed that GH triggers HIPK2 nuclear-cytoplasmic translocation, decreases HIPK2 binding to WIP1, and decreases ubiquitin binding to WIP1, concordant with GH-induced WIP1 expression. Indeed, immunocytochemistry showed that GH diminished HIPK2 expression and increased intranuclear WIP1.

Mechanisms of GH-induced WIP1 stabilization appear to involve AMPK. GH-induced AMPK phosphorylation prevented WIP1 phosphorylation and its degradation by HIPK2, as substantiated by blocking AMPK action to reduce WIP1 stability.

We further found that Src is involved in GH-induced WIP1 activation. By binding to GHR, GH activates Src,[13,21] and Src, in turn, mediates STAT5 phosphorylation in response to GH.[13,68] Transgenic mice overexpressing GH exhibit increased Src kinase activity,[69] and Src increases

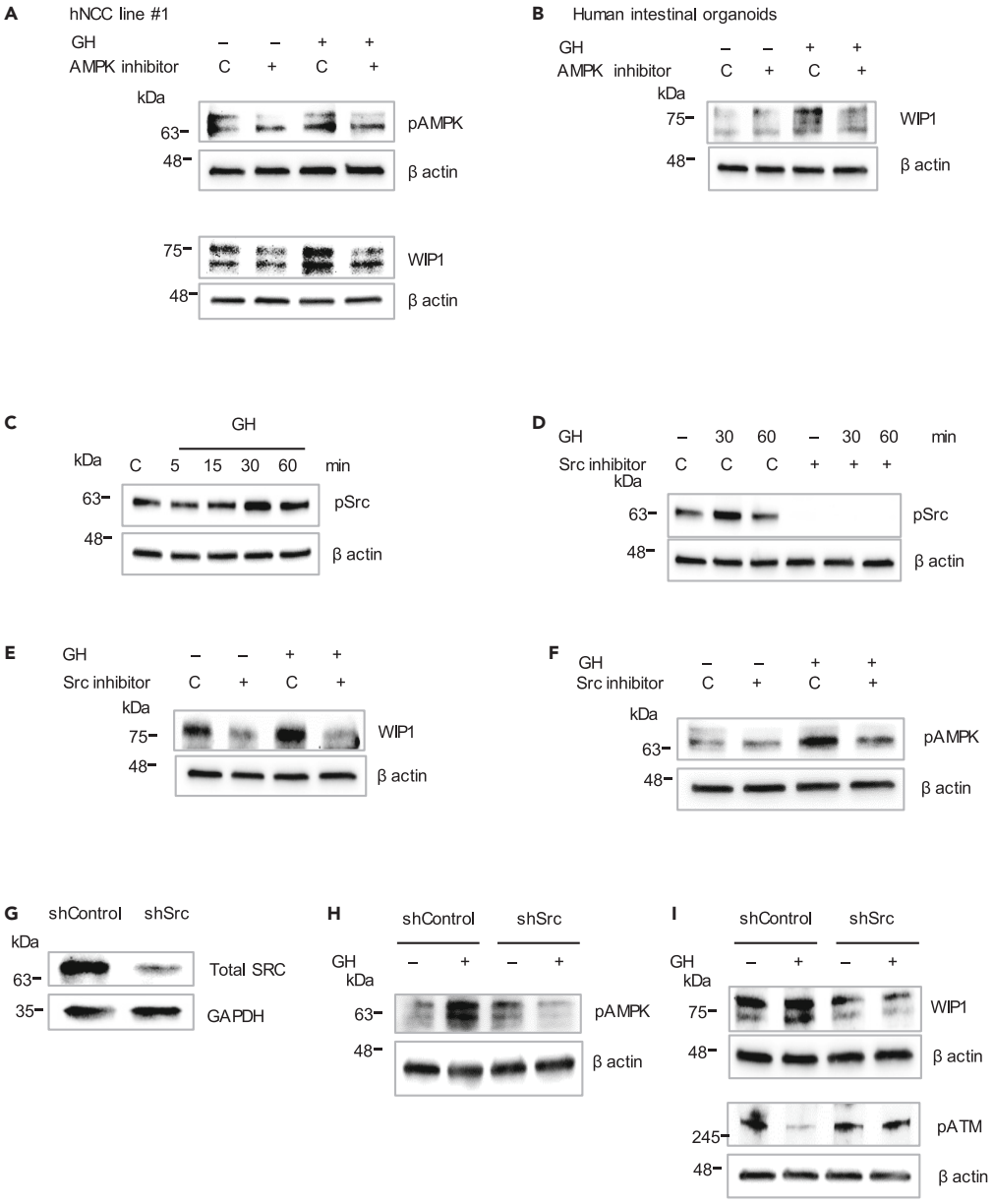

Figure 5. GH induces WIP1 by activating Src/AMPK

(A and B) Western blots of (A) hNCC line #1 treated with 1 μM AMPK inhibitor (Compound C) for 1 h followed by GH (500 ng/mL) for an additional 24 h and (B) human intestinal organoids treated with 2 μM AMPK inhibitor and GH (500 ng/mL) for 48 h.

(C–F) Western blots of hNCC line #1 was treated with (C) GH (500 ng/mL) for up to 60 min; (D) 25 μM Src inhibitor for 24 h followed by GH (500 ng/mL) for 30 min–60 min; (E) 25 μM Src inhibitor for 1 h followed by GH (500 ng/mL) for 24 h; and (F) 25 μM Src inhibitor for 24 h followed by GH (500 ng/mL) for 3 h. Untreated cells/organoids served as control (C).

(G–I) Western blots of hNCC line #1 transduced with lentivirus expressing Control shRNA (shControl) or Src shRNA (shSrc) (G) analyzed 72 h after transduction; (H) treated with GH (500 ng/mL) for 3 h; and (I) treated with GH (500 ng/mL) for 24 h. ImageJ quantifications of western blots are depicted in Figure S5.

AMPK phosphorylation and induces HIPK2 relocation to cytoplasm.[47,50] Our results indicate that GH-associated WIP1 induction is mediated by the Src/AMPK/HIPK2 pathway, as blocking Src action decreased AMPK phosphorylation, abolishing GH-induced WIP1.

In addition, HIPK2 is stabilized and activated in response to DNA damage through an ATM-dependent mechanism and initiates an apoptotic response by phosphorylating p53 at Ser 46.[70–72] Since ATM inactivation results in decreased HIPK2 activity,[70,71] GH-induced ATM suppression might diminish HIPK2 stability, which, in turn, could lead to WIP1 activation.

In acromegaly patients, increased peripheral lymphocyte chromosomal DNA damage points to suppressed DDR in response to GH excess.[73,74] Consistent with these observations, we show here that in peripheral blood buffy coats derived from acromegaly patients, high

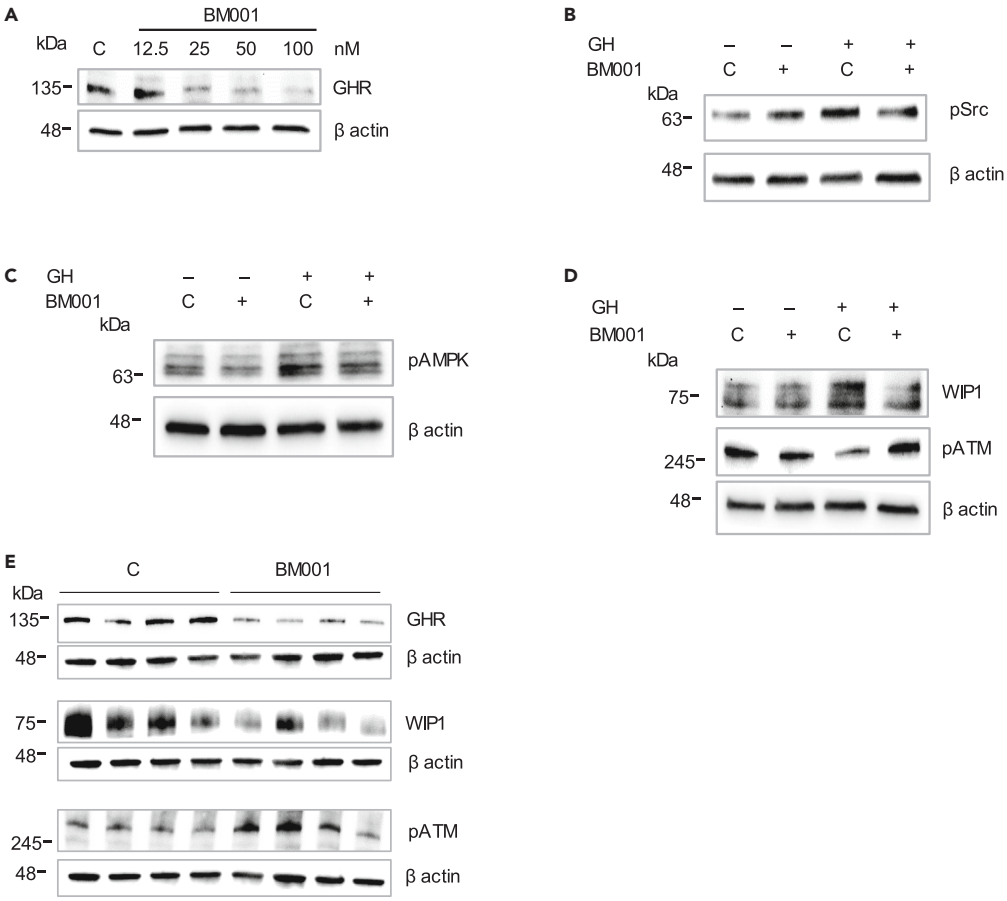

Figure 6. Blocking GH signaling inhibited GH-related WIP1 induction

(A–D) Western blots of hNCC line #1 treated with (A) increasing doses of BM001 (GHR synthesis inhibitor) for 24 h; (B) 25 nM BM001 for 24 h followed by GH (500 ng/mL) for 30 min; (C) 25 nM BM001 for 24 h followed by GH (500 ng/mL) for 3 h; and (D) 25 nM BM001 for 1 h followed by GH (500 ng/mL) for an additional 24 h.

(E) Colon tissue derived from 3-month-old female mice treated i.p. with DMSO (C, control) or BM001 (3 mg/kg) 3 times/week for 3 weeks. Mice were sacrificed 24 h after last injection. Each lane represents an individual animal. C, control. ImageJ quantifications of western blots are depicted in Figure S6.

WIP1 is associated with decreased ATM phosphorylation. As these patients are predisposed to colon polyps and other soft tissue growths and perhaps colorectal cancer,[27] our results identify a novel mechanism explaining these pathologies.

Overall, our results show a heretofore unappreciated GH signaling target. In addition to mediating skeletal growth largely by inducing IGF1, we show here that GH, by inducing Src/AMPK, downregulates HIPK2 activity, stabilizing WIP1 and suppressing phosphorylation of ATM, leading to accumulated unrepaired DNA (Figure 7). Identifying this GH signaling pathway mediated by WIP1 may offer new subcellular therapeutic targets to reverse adverse pathologies associated with DNA damage accumulation, including tissue degeneration associated with aging and neoplasm development.

Limitations of the study

The effects of GH on DDR mediated by WIP1 could be tissue specific. Although in this study GH induces WIP1 in colon cells and tissue as well as in buffy coat cells, it would be important to confirm GH actions on WIP1 in other tissue types. Importantly, we assessed GH effects in normal non-tumorous tissue and cells. It is not known whether GH affects WIP1 in malignant cells and tumors where DNA damage is very extensive. Also, as local GH is induced with age,[43] while pATM activity recedes with age,[75] it would be important to examine whether age-associated pATM and DNA damage repair decline is mediated by the GH/WIP1 pathway.

We demonstrated GH effects on WIP1 through the Src/AMPK pathway. However, although Src is induced 30 min after GH treatment, pAMPK increases 3 h later, and WIP1 is induced 24 h after GH treatment. It is clear, therefore, that additional intermediate pathways are likely involved in GH/Src/AMPK/WIP1 signaling. Thus, pAMPK directly phosphorylates several substrates,[76] including histone deacetylases. Accordingly, it would be of interest to delineate in further detail the sequential pathways involved in GH/WIP1 signaling.

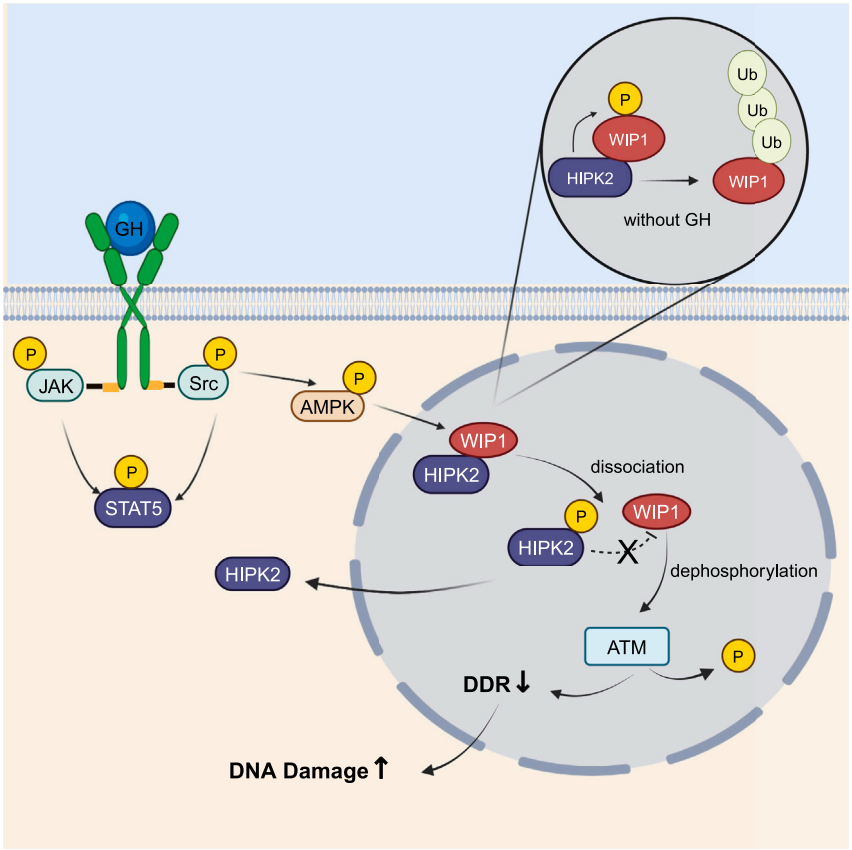

Figure 7. Proposed mechanisms for GH-mediated WIP1 induction

GH activates Src/AMPK phosphorylation. Phospho-AMPK, in turn, phosphorylates HIPK2, which is relocated to the cytoplasm, weakening binding to intranuclear WIP1, decreasing WIP1 ubiquitination, and increasing WIP1 stability. Induced WIP1 dephosphorylates ATM, thus suppressing DDR activity and leading to accumulated DNA damage. Created with BioRender.com.

STAR★METHODS

Detailed methods are provided in the online version of this paper and include the following:

- KEY RESOURCES TABLE
- RESOURCE AVAILABILITY
  - Lead contact
  - Materials availability
  - Data and code availability
- EXPERIMENTAL MODELS AND STUDY PARTICIPANT DETAILS
  - Study approval
  - Cell lines and treatments
  - 3D human intestinal organoids
  - GHR knockout mice
  - Xenograft model
  - Human blood samples
  - Constructs and transfections
- METHOD DETAILS
  - Treatments
  - Protein analysis
  - Immunoprecipitation
  - Immunocytochemistry
  - Comet assay
  - Real-time PCR

- Nucleofection
- QUANTIFICATION AND STATISTICAL ANALYSIS

SUPPLEMENTAL INFORMATION

Supplemental information can be found online at https://doi.org/10.1016/j.isci.2023.108117.

ACKNOWLEDGMENTS

Supported by NIH grants DK113998 and AG070211, Pfizer Award 61421295, and the Doris Factor Molecular Endocrinology Laboratory at Cedars-Sinai. The authors thank Specs Compound Handling BV and Peter Maas, PhD, for the supply of BM001; Catherine Bresee, MS, for assistance with statistical analysis; and Shira Berman for editorial assistance.

AUTHOR CONTRIBUTIONS

V.C. and S.M. developed the hypothesis. T.A., V.C., and S.M. wrote the manuscript. T.A., S.Z., C.Z., C.W.V., R.B., and V.C. conducted experiments. G.J.S. and J.A.M. developed GHR blocker BM001. T.A., S.Z., V.C., and S.M. analyzed, discussed, and interpreted the data. V.C. and S.M. coordinated and directed the project. All authors approved the submitted manuscript.

DECLARATION OF INTERESTS

The authors declare no competing interests.

Received: June 23, 2023
Revised: August 22, 2023
Accepted: September 29, 2023
Published: October 4, 2023

REFERENCES

1. Schiewer, M.J., and Knudsen, K.E. (2016). Linking DNA Damage and Hormone Signaling Pathways in Cancer. Trends Endocrinol. Metab. *27*, 216–225. https://doi.org/10.1016/j.tem.2016.02.004.
2. Ciccia, A., and Elledge, S.J. (2010). The DNA damage response: making it safe to play with knives. Mol. Cell *40*, 179–204. https://doi.org/10.1016/j.molcel.2010.09.019.
3. Chesnokova, V., and Melmed, S. (2020). Peptide Hormone Regulation of DNA Damage Responses. Endocr. Rev. *41*, bnaa009. https://doi.org/10.1210/endrev/bnaa009.
4. Blackford, A.N., and Jackson, S.P. (2017). ATM, ATR, and DNA-PK: The Trinity at the Heart of the DNA Damage Response. Mol. Cell *66*, 801–817. https://doi.org/10.1016/j.molcel.2017.05.015.
5. Bakkenist, C.J., and Kastan, M.B. (2003). DNA damage activates ATM through intermolecular autophosphorylation and dimer dissociation. Nature *421*, 499–506. https://doi.org/10.1038/nature01368.
6. Smith, J., Tho, L.M., Xu, N., and Gillespie, D.A. (2010). The ATM-Chk2 and ATR-Chk1 pathways in DNA damage signaling and cancer. Adv. Cancer Res. *108*, 73–112. https://doi.org/10.1016/b978-0-12-380888-2.00003-0.
7. Shiloh, Y., and Ziv, Y. (2013). The ATM protein kinase: regulating the cellular response to genotoxic stress, and more. Nat. Rev. Mol. Cell Biol. *14*, 197–210. https://doi.org/10.1038/nrm3546.
8. López-Otín, C., Blasco, M.A., Partridge, L., Serrano, M., and Kroemer, G. (2023). Hallmarks of aging: An expanding universe. Cell *186*, 243–278. https://doi.org/10.1016/j.cell.2022.11.001.
9. Kirkwood, T.B.L. (2005). Understanding the odd science of aging. Cell *120*, 437–447. https://doi.org/10.1016/j.cell.2005.01.027.
10. Harvey, S. (2010). Extrapituitary growth hormone. Endocrine *38*, 335–359. https://doi.org/10.1007/s12020-010-9403-8.
11. Chesnokova, V., Zhou, C., Ben-Shlomo, A., Zonis, S., Tani, Y., Ren, S.G., and Melmed, S. (2013). Growth hormone is a cellular senescence target in pituitary and nonpituitary cells. Proc. Natl. Acad. Sci. USA *110*, E3331–E3339. https://doi.org/10.1073/pnas.1310589110.
12. Chesnokova, V., Zonis, S., Barrett, R.J., Gleeson, J.P., and Melmed, S. (2019). Growth Hormone Induces Colon DNA Damage Independent of IGF-1. Endocrinology *160*, 1439–1447. https://doi.org/10.1210/en.2019-00132.
13. Dehkhoda, F., Lee, C.M.M., Medina, J., and Brooks, A.J. (2018). The Growth Hormone Receptor: Mechanism of Receptor Activation, Cell Signaling, and Physiological Aspects. Front. Endocrinol. *9*, 35. https://doi.org/10.3389/fendo.2018.00035.
14. Waters, M.J., Hoang, H.N., Fairlie, D.P., Pelekanos, R.A., and Brown, R.J. (2006). New insights into growth hormone action. J. Mol. Endocrinol. *36*, 1–7. https://doi.org/10.1677/jme.1.01933.
15. Brittain, A.L., Basu, R., Qian, Y., and Kopchick, J.J. (2017). Growth Hormone and the Epithelial-to-Mesenchymal Transition. J. Clin. Endocrinol. Metab. *102*, 3662–3673. https://doi.org/10.1210/jc.2017-01000.
16. Chesnokova, V., and Melmed, S. (2019). Growth hormone in the tumor microenvironment. Arch. Endocrinol. Metab. *63*, 568–575. https://doi.org/10.20945/2359-3997000000186.
17. Chesnokova, V., Zonis, S., Zhou, C., Recouvreux, M.V., Ben-Shlomo, A., Araki, T., Barrett, R., Workman, M., Wawrowsky, K., Ljubimov, V.A., et al. (2016). Growth hormone is permissive for neoplastic colon growth. Proc. Natl. Acad. Sci. USA *113*, E3250–E3259. https://doi.org/10.1073/pnas.1600561113.
18. Zhang, W., Qian, P., Zhang, X., Zhang, M., Wang, H., Wu, M., Kong, X., Tan, S., Ding, K., Perry, J.K., et al. (2015). Autocrine/Paracrine Human Growth Hormone-stimulated MicroRNA 96-182-183 Cluster Promotes Epithelial-Mesenchymal Transition and Invasion in Breast Cancer. J. Biol. Chem. *290*, 13812–13829. https://doi.org/10.1074/jbc.M115.653261.
19. Wang, J.J., Chong, Q.Y., Sun, X.B., You, M.L., Pandey, V., Chen, Y.J., Zhuang, Q.S., Liu, D.X., Ma, L., Wu, Z.S., et al. (2017). Autocrine hGH stimulates oncogenicity, epithelial-mesenchymal transition and cancer stem cell-like behavior in human colorectal carcinoma. Oncotarget *8*, 103900–103918. https://doi.org/10.18632/oncotarget.21812.
20. Chesnokova, V., Zonis, S., Barrett, R., Kameda, H., Wawrowsky, K., Ben-Shlomo, A., Yamamoto, M., Gleeson, J., Bresee, C., Gorbunova, V., and Melmed, S. (2019). Excess growth hormone suppresses DNA damage repair in epithelial cells. JCI Insight *4*, e125762. https://doi.org/10.1172/jci.insight.125762.
21. Boguszewski, C.L., and Boguszewski, M.C.d.S. (2019). Growth Hormone's Links to Cancer. Endocr. Rev. *40*, 558–574. https://doi.org/10.1210/er.2018-00166.
22. Chesnokova, V., and Melmed, S. (2023). Non-pituitary GH regulation of the epithelial microenvironment. Endocr. Relat. Cancer *30*, e230028. https://doi.org/10.1530/erc-23-0028.

23. Subramani, R., Nandy, S.B., Pedroza, D.A., and Lakshmanaswamy, R. (2017). Role of Growth Hormone in Breast Cancer. Endocrinology *158*, 1543–1555. https://doi.org/10.1210/en.2016-1928.
24. Kopchick, J.J., Basu, R., Berryman, D.E., Jorgensen, J.O.L., Johannsson, G., and Puri, V. (2022). Covert actions of growth hormone: fibrosis, cardiovascular diseases and cancer. Nat. Rev. Endocrinol. *18*, 558–573. https://doi.org/10.1038/s41574-022-00702-6.
25. Dal, J., Leisner, M.Z., Hermansen, K., Farkas, D.K., Bengtsen, M., Kistorp, C., Nielsen, E.H., Andersen, M., Feldt-Rasmussen, U., Dekkers, O.M., et al. (2018). Cancer Incidence in Patients With Acromegaly: A Cohort Study and Meta-Analysis of the Literature. J. Clin. Endocrinol. Metab. *103*, 2182–2188. https://doi.org/10.1210/jc.2017-02457.
26. Kasuki, L., Maia, B., and Gadelha, M.R. (2022). Acromegaly and Colorectal Neoplasm: An Update. Front. Endocrinol. *13*, 924952. https://doi.org/10.3389/fendo.2022.924952.
27. Melmed, S. (2009). Acromegaly pathogenesis and treatment. J. Clin. Invest. *119*, 3189–3202. https://doi.org/10.1172/jci39375.
28. Junnila, R.K., List, E.O., Berryman, D.E., Murrey, J.W., and Kopchick, J.J. (2013). The GH/IGF-1 axis in ageing and longevity. Nat. Rev. Endocrinol. *9*, 366–376. https://doi.org/10.1038/nrendo.2013.67.
29. Ikeno, Y., Bronson, R.T., Hubbard, G.B., Lee, S., and Bartke, A. (2003). Delayed occurrence of fatal neoplastic diseases in ames dwarf mice: correlation to extended longevity. J. Gerontol. A Biol. Sci. Med. Sci. *58*, 291–296. https://doi.org/10.1093/gerona/58.4.b291.
30. Carroll, R.E., Goodlad, R.A., Poole, A.J., Tyner, A.L., Robey, R.B., Swanson, S.M., and Unterman, T.G. (2009). Reduced susceptibility to azoxymethane-induced aberrant crypt foci formation and colon cancer in growth hormone deficient rats. Growth Horm. IGF Res. *19*, 447–456. https://doi.org/10.1016/j.ghir.2009.02.001.
31. Duran-Ortiz, S., List, E.O., Ikeno, Y., Young, J., Basu, R., Bell, S., McHugh, T., Funk, K., Mathes, S., Qian, Y., et al. (2021). Growth hormone receptor gene disruption in mature-adult mice improves male insulin sensitivity and extends female lifespan. Aging Cell *20*, e13506. https://doi.org/10.1111/acel.13506.
32. Ikeno, Y., Hubbard, G.B., Lee, S., Cortez, L.A., Lew, C.M., Webb, C.R., Berryman, D.E., List, E.O., Kopchick, J.J., and Bartke, A. (2009). Reduced incidence and delayed occurrence of fatal neoplastic diseases in growth hormone receptor/binding protein knockout mice. J. Gerontol. A Biol. Sci. Med. Sci. *64*, 522–529. https://doi.org/10.1093/gerona/glp017.
33. Guevara-Aguirre, J., Balasubramanian, P., Guevara-Aguirre, M., Wei, M., Madia, F., Cheng, C.W., Hwang, D., Martin-Montalvo, A., Saavedra, J., Ingles, S., et al. (2011). Growth hormone receptor deficiency is associated with a major reduction in pro-aging signaling, cancer, and diabetes in humans. Sci. Transl. Med. *3*, 70ra13. .. https://doi.org/10.1126/scitranslmed.3001845
34. Shevah, O., and Laron, Z. (2007). Patients with congenital deficiency of IGF-I seem protected from the development of malignancies: a preliminary report. Growth Horm. IGF Res. *17*, 54–57. https://doi.org/10.1016/j.ghir.2006.10.007.
35. Werner, H., Lapkina-Gendler, L., Achlaug, L., Nagaraj, K., Somri, L., Yaron-Saminsky, D., Pasmanik-Chor, M., Sarfstein, R., Laron, Z., and Yakar, S. (2019). Genome-Wide Profiling of Laron Syndrome Patients Identifies Novel Cancer Protection Pathways. Cells *8*. https://doi.org/10.3390/cells8060596.
36. Qian, Y., Berryman, D.E., Basu, R., List, E.O., Okada, S., Young, J.A., Jensen, E.A., Bell, S.R.C., Kulkarni, P., Duran-Ortiz, S., et al. (2022). Mice with gene alterations in the GH and IGF family. Pituitary *25*, 1–51. https://doi.org/10.1007/s11102-021-01191-y.
37. Lu, X., Nguyen, T.A., Moon, S.H., Darlington, Y., Sommer, M., and Donehower, L.A. (2008). The type 2C phosphatase Wip1: an oncogenic regulator of tumor suppressor and DNA damage response pathways. Cancer Metastasis Rev. *27*, 123–135. https://doi.org/10.1007/s10555-008-9127-x.
38. Shreeram, S., Demidov, O.N., Hee, W.K., Yamaguchi, H., Onishi, N., Kek, C., Timofeev, O.N., Dudgeon, C., Fornace, A.J., Anderson, C.W., et al. (2006). Wip1 phosphatase modulates ATM-dependent signaling pathways. Mol. Cell *23*, 757–764. https://doi.org/10.1016/j.molcel.2006.07.010.
39. Bulavin, D.V., Phillips, C., Nannenga, B., Timofeev, O., Donehower, L.A., Anderson, C.W., Appella, E., and Fornace, A.J., Jr. (2004). Inactivation of the Wip1 phosphatase inhibits mammary tumorigenesis through p38 MAPK-mediated activation of the p16(Ink4a)-p19(Arf) pathway. Nat. Genet. *36*, 343–350. https://doi.org/10.1038/ng1317.
40. Peng, T.S., He, Y.H., Nie, T., Hu, X.D., Lu, H.Y., Yi, J., Shuai, Y.F., and Luo, M. (2014). PPM1D is a prognostic marker and therapeutic target in colorectal cancer. Exp. Ther. Med. *8*, 430–434. https://doi.org/10.3892/etm.2014.1762.
41. Choi, D.W., Na, W., Kabir, M.H., Yi, E., Kwon, S., Yeom, J., Ahn, J.W., Choi, H.H., Lee, Y., Seo, K.W., et al. (2013). WIP1, a homeostatic regulator of the DNA damage response, is targeted by HIPK2 for phosphorylation and degradation. Mol. Cell *51*, 374–385. https://doi.org/10.1016/j.molcel.2013.06.010.
42. Fiscella, M., Zhang, H., Fan, S., Sakaguchi, K., Shen, S., Mercer, W.E., Vande Woude, G.F., O'Connor, P.M., and Appella, E. (1997). Wip1, a novel human protein phosphatase that is induced in response to ionizing radiation in a p53-dependent manner. Proc. Natl. Acad. Sci. USA *94*, 6048–6053. https://doi.org/10.1073/pnas.94.12.6048.
43. Chesnokova, V., Zonis, S., Apostolou, A., Estrada, H.Q., Knott, S., Wawrowsky, K., Michelsen, K., Ben-Shlomo, A., Barrett, R., Gorbunova, V., et al. (2021). Local non-pituitary growth hormone is induced with aging and facilitates epithelial damage. Cell Rep. *37*, 110068. https://doi.org/10.1016/j.celrep.2021.110068.
44. Gilmartin, A.G., Faitg, T.H., Richter, M., Groy, A., Seefeld, M.A., Darcy, M.G., Peng, X., Federowicz, K., Yang, J., Zhang, S.Y., et al. (2014). Allosteric Wip1 phosphatase inhibition through flap-subdomain interaction. Nat. Chem. Biol. *10*, 181–187. https://doi.org/10.1038/nchembio.1427.
45. Wook Choi, D., and Yong Choi, C. (2014). HIPK2 modification code for cell death and survival. Mol. Cell. Oncol. *1*, e955999. https://doi.org/10.1080/23723548.2014.955999.
46. Bain, J., Plater, L., Elliott, M., Shpiro, N., Hastie, C.J., McLauchlan, H., Klevernic, I., Arthur, J.S.C., Alessi, D.R., and Cohen, P. (2007). The selectivity of protein kinase inhibitors: a further update. Biochem. J. *408*, 297–315. https://doi.org/10.1042/bj20070797.
47. Polonio-Vallon, T., Kirkpatrick, J., Krijgsveld, J., and Hofmann, T.G. (2014). Src kinase modulates the apoptotic p53 pathway by altering HIPK2 localization. Cell Cycle *13*, 115–125. https://doi.org/10.4161/cc.26857.
48. Xie, Z., Dong, Y., Scholz, R., Neumann, D., and Zou, M.H. (2008). Phosphorylation of LKB1 at serine 428 by protein kinase C-zeta is required for metformin-enhanced activation of the AMP-activated protein kinase in endothelial cells. Circulation *117*, 952–962. https://doi.org/10.1161/circulationaha.107.744490.
49. Mizrachy-Schwartz, S., Kravchenko-Balasha, N., Ben-Bassat, H., Klein, S., and Levitzki, A. (2007). Optimization of energy-consuming pathways towards rapid growth in HPV-transformed cells. PLoS One *2*, e628. https://doi.org/10.1371/journal.pone.0000628.
50. Mizrachy-Schwartz, S., Cohen, N., Klein, S., Kravchenko-Balasha, N., and Levitzki, A. (2011). Up-regulation of AMP-activated protein kinase in cancer cell lines is mediated through c-Src activation. J. Biol. Chem. *286*, 15268–15277. https://doi.org/10.1074/jbc.M110.211813.
51. Zhu, T., Ling, L., and Lobie, P.E. (2002). Identification of a JAK2-independent pathway regulating growth hormone (GH)-stimulated p44/42 mitogen-activated protein kinase activity. GH activation of Ral and phospholipase D is Src-dependent. J. Biol. Chem. *277*, 45592–45603. https://doi.org/10.1074/jbc.M201385200.
52. van der Velden, L.M., Maas, P., van Amersfoort, M., Timmermans-Sprang, E.P.M., Mensinga, A., van der Vaart, E., Malergue, F., Viëtor, H., Derksen, P.W.B., Klumperman, J., et al. (2022). Small molecules to regulate the GH/IGF1 axis by inhibiting the growth hormone receptor synthesis. Front. Endocrinol. *13*, 926210. https://doi.org/10.3389/fendo.2022.926210.
53. Bartek, J., Bartkova, J., and Lukas, J. (2007). DNA damage signalling guards against activated oncogenes and tumour progression. Oncogene *26*, 7773–7779. https://doi.org/10.1038/sj.onc.1210881.
54. Bartkova, J., Rezaei, N., Liontos, M., Karakaidos, P., Kletsas, D., Issaeva, N., Vassiliou, L.V.F., Kolettas, E., Niforou, K., Zoumpourlis, V.C., et al. (2006). Oncogene-induced senescence is part of the tumorigenesis barrier imposed by DNA damage checkpoints. Nature *444*, 633–637. https://doi.org/10.1038/nature05268.
55. Negrini, S., Gorgoulis, V.G., and Halazonetis, T.D. (2010). Genomic instability — an evolving hallmark of cancer. Nat. Rev. Mol. Cell Biol. *11*, 220–228. https://doi.org/10.1038/nrm2858.
56. Lord, C.J., and Ashworth, A. (2012). The DNA damage response and cancer therapy. Nature *481*, 287–294. https://doi.org/10.1038/nature10760.
57. Halazonetis, T.D., Gorgoulis, V.G., and Bartek, J. (2008). An oncogene-induced DNA damage model for cancer development. Science *319*, 1352–1355. https://doi.org/10.1126/science.1140735.
58. Nannenga, B., Lu, X., Dumble, M., Van Maanen, M., Nguyen, T.A., Sutton, R., Kumar, T.R., and Donehower, L.A. (2006). Augmented cancer resistance and DNA damage response phenotypes in PPM1D null mice. Mol. Carcinog. *45*, 594–604. https://doi.org/10.1002/mc.20195.
59. Darlington, Y., Nguyen, T.A., Moon, S.H., Herron, A., Rao, P., Zhu, C., Lu, X., and

Donehower, L.A. (2012). Absence of Wip1 partially rescues Atm deficiency phenotypes in mice. Oncogene *31*, 1155–1165. https://doi.org/10.1038/onc.2011.303.

60. Kleinberg, D.L., Wood, T.L., Furth, P.A., and Lee, A.V. (2009). Growth hormone and insulin-like growth factor-I in the transition from normal mammary development to preneoplastic mammary lesions. Endocr. Rev. *30*, 51–74. https://doi.org/10.1210/er.2008-0022.
61. Nakonechnaya, A.O., Jefferson, H.S., Chen, X., and Shewchuk, B.M. (2013). Differential effects of exogenous and autocrine growth hormone on LNCaP prostate cancer cell proliferation and survival. J. Cell. Biochem. *114*, 1322–1335. https://doi.org/10.1002/jcb.24473.
62. Clayton, P.E., Banerjee, I., Murray, P.G., and Renehan, A.G. (2011). Growth hormone, the insulin-like growth factor axis, insulin and cancer risk. Nat. Rev. Endocrinol. *7*, 11–24. https://doi.org/10.1038/nrendo.2010.171.
63. Miquet, J.G., Freund, T., Martinez, C.S., González, L., Díaz, M.E., Micucci, G.P., Zotta, E., Boparai, R.K., Bartke, A., Turyn, D., and Sotelo, A.I. (2013). Hepatocellular alterations and dysregulation of oncogenic pathways in the liver of transgenic mice overexpressing growth hormone. Cell Cycle *12*, 1042–1057. https://doi.org/10.4161/cc.24026.
64. Törnell, J., Carlsson, B., Pohjanen, P., Wennbo, H., Rymo, L., and Isaksson, O. (1992). High frequency of mammary adenocarcinomas in metallothionein promoter-human growth hormone transgenic mice created from two different strains of mice. J. Steroid Biochem. Mol. Biol. *43*, 237–242. https://doi.org/10.1016/0960-0760(92)90213-3.
65. Snibson, K.J., Bhathal, P.S., and Adams, T.E. (2001). Overexpressed growth hormone (GH) synergistically promotes carcinogen-initiated liver tumour growth by promoting cellular proliferation in emerging hepatocellular neoplasms in female and male GH-transgenic mice. Liver *21*, 149–158. https://doi.org/10.1034/j.1600-0676.2001.021002149.x.
66. D'Orazi, G., Sciulli, M.G., Di Stefano, V., Riccioni, S., Frattini, M., Falcioni, R., Bertario, L., Sacchi, A., and Patrignani, P. (2006). Homeodomain-interacting protein kinase-2 restrains cytosolic phospholipase A2-dependent prostaglandin E2 generation in human colorectal cancer cells. Clin. Cancer Res. *12*, 735–741. https://doi.org/10.1158/1078-0432.CCR-05-1557.
67. Sombroek, D., and Hofmann, T.G. (2009). How cells switch HIPK2 on and off. Cell Death Differ. *16*, 187–194. https://doi.org/10.1038/cdd.2008.154.
68. Manabe, N., Kubota, Y., Kitanaka, A., Ohnishi, H., Taminato, T., and Tanaka, T. (2006). Src transduces signaling via growth hormone (GH)-activated GH receptor (GHR) tyrosine-phosphorylating GHR and STAT5 in human leukemia cells. Leuk. Res. *30*, 1391–1398. https://doi.org/10.1016/j.leukres.2006.03.024.
69. Miquet, J.G., González, L., Matos, M.N., Hansen, C.E., Louis, A., Bartke, A., Turyn, D., and Sotelo, A.I. (2008). Transgenic mice overexpressing GH exhibit hepatic upregulation of GH-signaling mediators involved in cell proliferation. J. Endocrinol. *198*, 317–330. https://doi.org/10.1677/joe-08-0002.
70. Dauth, I., Krüger, J., and Hofmann, T.G. (2007). Homeodomain-interacting protein kinase 2 is the ionizing radiation-activated p53 serine 46 kinase and is regulated by ATM. Cancer Res. *67*, 2274–2279. https://doi.org/10.1158/0008-5472.CAN-06-2884.
71. Winter, M., Sombroek, D., Dauth, I., Moehlenbrink, J., Scheuermann, K., Crone, J., and Hofmann, T.G. (2008). Control of HIPK2 stability by ubiquitin ligase Siah-1 and checkpoint kinases ATM and ATR. Nat. Cell Biol. *10*, 812–824. https://doi.org/10.1038/ncb1743.
72. Hofmann, T.G., Möller, A., Sirma, H., Zentgraf, H., Taya, Y., Dröge, W., Will, H., and Schmitz, M.L. (2002). Regulation of p53 activity by its interaction with homeodomain-interacting protein kinase-2. Nat. Cell Biol. *4*, 1–10. https://doi.org/10.1038/ncb715.
73. Bayram, F., Bitgen, N., Donmez-Altuntas, H., Cakir, I., Hamurcu, Z., Sahin, F., Simsek, Y., and Baskol, G. (2014). Increased genome instability and oxidative DNA damage and their association with IGF-1 levels in patients with active acromegaly. Growth Horm. IGF Res. *24*, 29–34. https://doi.org/10.1016/j.ghir.2013.12.002.
74. Unal, O.K., Cinkilic, N., Gul, O.O., Cander, S., Vatan, O., Ersoy, C., Yilmaz, D., and Tuncel, E. (2014). Investigation of genotoxicity in acromegaly from peripheral blood lymphocyte cultures using a micronucleus assay. J. Clin. Endocrinol. Metab. *99*, E2060–E2066. https://doi.org/10.1210/jc.2014-1641.
75. Gutierrez-Martinez, P., Hogdal, L., Nagai, M., Kruta, M., Singh, R., Sarosiek, K., Nussenzweig, A., Beerman, I., Letai, A., and Rossi, D.J. (2018). Diminished apoptotic priming and ATM signalling confer a survival advantage onto aged haematopoietic stem cells in response to DNA damage. Nat. Cell Biol. *20*, 413–421. https://doi.org/10.1038/s41556-018-0054-y.
76. Mihaylova, M.M., and Shaw, R.J. (2011). The AMPK signalling pathway coordinates cell growth, autophagy and metabolism. Nat. Cell Biol. *13*, 1016–1023. https://doi.org/10.1038/ncb2329.
77. Barrett, R., Ornelas, L., Yeager, N., Mandefro, B., Sahabian, A., Lenaeus, L., Targan, S.R., Svendsen, C.N., and Sareen, D. (2014). Reliable generation of induced pluripotent stem cells from human lymphoblastoid cell lines. Stem Cells Transl. Med. *3*, 1429–1434. https://doi.org/10.5966/sctm.2014-0121.
78. Workman, M.J., Gleeson, J.P., Troisi, E.J., Estrada, H.Q., Kerns, S.J., Hinojosa, C.D., Hamilton, G.A., Targan, S.R., Svendsen, C.N., and Barrett, R.J. (2018). Enhanced Utilization of Induced Pluripotent Stem Cell-Derived Human Intestinal Organoids Using Microengineered Chips. Cell. Mol. Gastroenterol. Hepatol. *5*, 669–677.e2. https://doi.org/10.1016/j.jcmgh.2017.12.008.
79. Melmed, S. (2020). Pituitary-Tumor Endocrinopathies. N. Engl. J. Med. *382*, 937–950. https://doi.org/10.1056/NEJMra1810772.
80. Sadowski, C.L., Wheeler, T.T., Wang, L.H., and Sadowski, H.B. (2001). GH regulation of IGF-I and suppressor of cytokine signaling gene expression in C2C12 skeletal muscle cells. Endocrinology *142*, 3890–3900. https://doi.org/10.1210/endo.142.9.8365.
81. Herrington, J., Smit, L.S., Schwartz, J., and Carter-Su, C. (2000). The role of STAT proteins in growth hormone signaling. Oncogene *19*, 2585–2597. https://doi.org/10.1038/sj.onc.1203526.
82. Schneider, A., Wood, H.N., Geden, S., Greene, C.J., Yates, R.M., Masternak, M.M., and Rohde, K.H. (2019). Growth hormone-mediated reprogramming of macrophage transcriptome and effector functions. Sci. Rep. *9*, 19348. https://doi.org/10.1038/s41598-019-56017-6.
83. Kofoed, E.M., Hwa, V., Little, B., Woods, K.A., Buckway, C.K., Tsubaki, J., Pratt, K.L., Bezrodnik, L., Jasper, H., Tepper, A., et al. (2003). Growth hormone insensitivity associated with a STAT5b mutation. N. Engl. J. Med. *349*, 1139–1147. https://doi.org/10.1056/NEJMoa022926.
84. Okada, S., and Kopchick, J.J. (2001). Biological effects of growth hormone and its antagonist. Trends Mol. Med. *7*, 126–132. https://doi.org/10.1016/s1471-4914(01)01933-5.
85. Kopchick, J.J. (2003). Discovery and mechanism of action of pegvisomant. Eur. J. Endocrinol. *148* (*Suppl 2*), S21–S25. https://doi.org/10.1530/eje.0.148s021.

STAR★METHODS

KEY RESOURCES TABLE

REAGENT or RESOURCE	SOURCE	IDENTIFIER
Antibodies		
Rabbit anti-Phospho-ATM (Ser1981)	Cell Signaling Technology	Cat# 13050; RRID: AB_2798100
Rabbit anti-Phospho-ATM (Ser1981)	R&D Systems	Cat# AF1655
Rabbit anti-ATM	Abcam	Cat# ab82512; RRID: AB_2040568
Rabbit anti-Phospho-Histone H2A.X (Ser139)	Cell Signaling Technology	Cat# 9718; RRID: AB_10121789
Mouse anti-Phosho-p53 (Ser15) (clone 16G8)	Cell Signaling Technology	Cat# 9286; RRID: AB_331741
Goat anti-p53	R&D Systems	Cat# AF1355
Rabbit anti-Phospho-Chk2 (Thr68)	Cell Signaling Technology	Cat# 2661S; RRID: AB_331479
Rabbit anti-GAPDH (14C10)	Cell Signaling Technology	Cat# 2118; RRID: AB_561053
Rabbit anti-WIP1 (D-4F7)	Cell Signaling Technology	Cat# 11901; RRID: AB_2797762
Rabbit anti-WIP1	LSBio	Cat# LS-C101018
Mouse anti-WIP1 (F-10)	Santa Cruz Biotechnology	Cat# sc-376257; RRID: AB_10986000
Mouse anti-Ubiquitin (A-5)	Santa Cruz Biotechnology	Cat# sc-166553; RRID: AB_2241297
Mouse anti-*c*-Src (H-12)	Santa Cruz Biotechnology	Cat# sc-5266; RRID: AB_627308
Rabbit anti-Lamin A/C (H-110)	Santa Cruz Biotechnology	Cat# sc-20681; RRID: AB_648154
Mouse anti-HIPK2 (F-189)	Santa Cruz Biotechnology	Cat# sc-100383; RRID: AB_1124683
Goat Anti-GHR	R&D Systems	Cat# AF1210
Rabbit anti-HIPK2	ThermoFisher Scientific	Cat# PA5-40567; RRID: AB_2605444
Mouse anti-HIPK2	Active Motif	Cat# 39677; RRID: AB_2615043
Rabbit anti-Phospho-AMPK alpha-1,2 (Thr183, Thr172)	ThermoFisher Scientific	Cat# PA5-17831; RRID: AB_10983715
Rabbit anti-Phospho-Src (Y416)	R&D Systems	Cat# MAB2685
Goat anti-Growth Hormone	R&D Systems	Cat# AF1067; RRID: AB_354573
Rabbit anti-Growth Hormone	LS Bio	Cat# LS-B4199; RRID: AB_10719011
Mouse anti-Beta-actin (clone AC-15)	Sigma-Aldrich	Cat# A1978; RRID: AB_476692
Mouse IgG	Santa Cruz Biotechnology	Cat# sc-2025; RRID: AB_737182
ECL anti-mouse IgG, HRP, made in sheep	GE Healthcare Life Sciences	Cat# NA931; RRID: AB_772210
ECL anti-rabbit IgG, HRP, made in sheep	GE Healthcare Life Sciences	Cat# NA934; RRID: AB_772206
ECL Donkey anti-goat IgG, HRP	Jackson ImmunoResearch	Cat# 805-035-180; RRID: AB_2340874
Alexa Fluor 568 donkey anti-rabbit IgG	Thermo Fisher Scientific	Cat# A-10042; RRID: AB_2534017
Alexa Fluor 488 donkey anti-mouse IgG	Thermo Fisher Scientific	Cat# A-21202; RRID: AB_141607
Alexa Fluor 647 Phalloidin	Thermo Fisher Scientific	Cat# A-22287
Bacterial and virus strains		
pLV-EF1p-hGH1-IRES-eGFP-WPRE lentiviral particles	Regenerative Medicine Institute at Cedars-Sinai Medical Center	N/A
pLV-EF1p-mCherry-IRES-eGFP-WPRE lentiviral particles	Regenerative Medicine Institute at Cedars-Sinai Medical Center	N/A
EF1-luc2-mGH-Ubic lentiviral particles	Regenerative Medicine Institute at Cedars-Sinai Medical Center	N/A
EF1-luc2-Ubic lentiviral control particles	Regenerative Medicine Institute at Cedars-Sinai Medical Center	N/A
GH1 shRNA (human) lentiviral particles	Santa Cruz Biotechnology	Cat# sc-43803-V
Src shRNA (human) lentiviral particles	Santa Cruz Biotechnology	Cat# sc-29228-V

(*Continued on next page*)

Continued

REAGENT or RESOURCE	SOURCE	IDENTIFIER
Control shRNA lentiviral particles - A	Santa Cruz Biotechnology	Cat# sc-108080
Chemicals, peptides, and recombinant proteins		
Etoposide	Sigma-Aldrich	Cat# E1383
Pegvisomant (Somavert)	Pfizer	LAB-0782-2.0
GSK2830371	MilliporeSigma	Cat# SML1048
Compound C (CAS 866405-64-3)	MilliporeSigma	Cat# 171260
Dasatinib (BMS-354825)	Selleck Chemicals	Cat# S1021
BM001	Specs	N/A
Human recombinant GH	BioVision	Cat# 4769-500
Activin A	R&D systems	Cat# 338-AC
Wnt3A	R&D systems	Cat# 5036-WN
CHIR 99021	Tocris	Cat# 4423/10
FGF4	R&D systems	Cat# 2035-F4
Noggin	R&D systems	Cat# 6057-NG
Matrigel	Corning	Cat# 354234
EGF	R&D systems	Cat# 236-EG
B-27	Thermo Fisher Scientific	Cat# 17504044
A83301	Tocris	Cat# 2939
SB 202190	Tocris	Cat# 1264
TrypLE	Thermo Fisher Scientific	Cat# 12604013
Cell Recovery Solution	Corning	Cat# 354253
IntestiCult Organoid Growth Medium	STEMCELL Technologies	Cat# 06010
PriGrow III media	Applied Biological Materials	Cat# TM003
DMEM/F12 media	Invitrogen	Cat# 11320033
McCoy's 5A medium	Invitrogen	Cat#16600082
Antibiotic:antimycotic (anti:anti) solution	Gemini Bio-Products	Cat# 400-101
Hydrocortisone	Sigma-Aldrich	Cat# H4001
Insulin solution human	Sigma-Aldrich	Cat# I9278
Donor horse serum	Omega Scientific	Cat# DH-05
Halt™ Protease and Phosphatase Inhibitor Cocktail (100X)	ThermoFisher Scientific	Cat# 78440
Protease inhibitor cocktail	MilliporeSigma	Cat# P8340
RIPA buffer	Cell Signaling	Cat #9806S
Polybrene	Santa Cruz Biotechnology	Cat# sc-134220
Trizol	Invitrogen	Cat# 15596018
Histopaque 1077 solution	MilliporeSigma	Cat# H8889
SsoAdvanced Universal SYBR Green SuperMix	Bio-Rad Laboratories	Cat# 1725274
Hikari Signal Enhancer Kit for primary and secondary antibody	Nacalai USA	Cat# NU00102
Critical commercial assays		
Human GH ELISA kit	ALPCO	Cat# 25-HGHHU-E01
Mouse GH ELISA kit	MilliporeSigma	Cat# EZRMGH-45K
DC Protein Assay Kit	Bio-Rad	Cat# 5000112
NE-PER Nuclear and cytoplasmic Extraction Reagents	Thermo Fisher Scientific	Cat# 78833
Protein G Immunoprecipitation Kit	Sigma-Aldrich	Cat# IP50

(*Continued on next page*)

Continued

REAGENT or RESOURCE	SOURCE	IDENTIFIER
SuperScript II First-Strand cDNA synthesis system	Thermo Fisher Scientific	Cat# 18091050
RNAeasy mini Kit	Qiagen	Cat# 74104
First-Strand cDNA synthesis system	Thermo Fisher Scientific	Cat# 18091050
OxiSelect Comet Assay Kit	Cell Biolabs	Cat# STA-350
Experimental models: Cell lines		
HCT116	ATCC	Cat# CCL-247; RRID: CVCL_0291
Human normal colon cells derived from biopsy (hNCC), line#1	Applied Biological Materials	Cat# T4056, lot# HC1211
Human normal colon cells derived from biopsy (hNCC), line#2	Applied Biological Materials	Cat# T4056, lot# 0145834955002
MCF12A	ATCC	Cat# CRL-10782
iPSC line Edi029 generated from human peripheral blood mononuclear cells (line#1)	Regenerative Medicine Institute at Cedars-Sinai Medical Center	N/A
iPSC line 03i generated from human fibroblasts (line#2)	Regenerative Medicine Institute at Cedars-Sinai Medical Center	N/A
iPSC line 688i generated from human lymphoblastoids (line#3)	Regenerative Medicine Institute at Cedars-Sinai Medical Center	N/A
Experimental models: Organisms/strains		
Mouse: C57BL/6J	The Jackson Laboratory	Stock ID#00064; RRID: IMSR_JAX:000664
Mouse: B6N[Cg]-Ghr <tm1b(KOMP)Wtsi>/3J	The Jackson Laboratory	Stock ID# 021486
Mouse: NU/J	The Jackson Laboratory	Strain# 002019 RRID: IMSR_JAX:002019
Oligonucleotides		
WIP1 siRNA (human)	Santa Cruz Biotechnology	Cat# sc-39205
Control siRNA-A	Santa Cruz Biotechnology	Cat# sc-37007
PrimePCR Assay PPM1D, Hsa	Bio-Rad laboratories	Cat# 10025636 qHsaCID0016220
PrimePCR Assay GAPDH, Hsa	Bio-Rad laboratories	Cat# 1002563 qHsaCED0038674
Software and algorithms		
GraphPad Prism 9	GraphPad Software	https://www.graphpad.com/scientific-software/prism/
ImageJ	NIH	https://ImageJ.nih.gov/ij/
CFX Maestro 1.0	Bio-Rad Laboratories	Cat# 12004110
Image Lab	Bio-Rad Laboratories	Cat# 17006130
Other		
Trans-Blot Turbo Transfer System	Bio-Rad Laboratories	Cat# 1704150
Molecular Imager ChemiDoc XRS Plus Imaging System	Bio-Rad Laboratories	Cat# 1708265
CFX96 Touch Real-Time PCR System	Bio-Rad Laboratories	Cat# 1845096
S1000 Thermal Cycler	Bio-Rad Laboratories	Cat# 1852148
FACSAria cell sorter	BD Biosciences	N/A
FACS-Canto	BD Biosciences	N/A
OPTICA IM-3LD2 Trinocular Inverted LED Epi-Fluorescence Microscope	Leica Microsystems	Cat# OPIM-3LD2
Stellaris Confocal Microscope	Leica Microsystems	https://www.leica-microsystems.com/ppc/confocal

RESOURCE AVAILABILITY

Lead contact

- Further information and requests for resources and reagents should be directed to and will be fulfilled by the lead contact, Shlomo Melmed (melmed@csmc.edu).

Materials availability

- This study did not generate new unique reagents.

Data and code availability

- The data reported in this study are available in this paper and its supplemental information.
- This paper does not report original code.
- Any additional information required to reanalyze the data reported in this paper is available from the lead contact upon request.

EXPERIMENTAL MODELS AND STUDY PARTICIPANT DETAILS

Study approval

Animal experiments were approved by the Cedars-Sinai Institutional Animal Care and Use Committee (IACUC #009252). The generation of iPSCs obtained from healthy human volunteer donors at Cedars-Sinai was approved by the Cedars-Sinai Medical Center Institutional Review Board (IRB #40182). Informed consent was obtained for use of blood samples from patients before pituitary adenoma surgical resection per the Cedars-Sinai Institutional Review Board (IRB #2873).

Cell lines and treatments

hNCC line #1 and line #2 were isolated from normal colon sections of two de-identified individuals and validated as cytokeratin 18- and 19-expressing colon epithelial cells. Tissue donor sex and age are unavailable. Cells were grown at 37°C and 5% CO_2 in PriGrow III Medium supplemented with 5% FBS, and with antibiotic/antimycotic solution from Gemini Bio-Products, then transduced with lentivirus or treated before passage 15. MCF12A were cultured in DMEM/F12 with 0.5 μg/mL hydrocortisone, 10 μg/mL insulin, 20 ng/mL EGF, 5% horse serum, and antibiotic/antimycotic solution. Human colon carcinoma HCT116 cells were obtained from ATCC and cultured in McCoy's 5A medium supplemented with 10% FBS and with antibiotic/antimycotic solution.

3D human intestinal organoids

Three iPSC lines (CS03iCTR-n1, CS688iCTR-n5, and Edi029-A) obtained from the Cedars-Sinai iPSC Core were derived from fibroblasts or human lymphoblastoid cell lines or peripheral blood mononuclear cells from de-identified healthy volunteer donors. Cell lines were fully characterized for pluripotency markers, confirmed to be karyotypically normal, and maintained in an undifferentiated state on Matrigel-coated plates in mTeSR1 media under feeder-free conditions.

Generation and culturing of intestinal organoids were performed as described.[77,78] Three-dimensional intestinal organoids were generated from iPSC lines using episomal plasmid reprogramming. To induce definitive endoderm formation, iPSCs were cultured with activin A (100 ng/mL) with increasing concentrations of FBS (0%, 0.2%, and 2% on days 1, 2, and 3, respectively). Wnt3A (25 ng/mL) was also added on the first day of endoderm differentiation. To induce hindgut formation, cells were cultured in Advanced DMEM/F12 with 2% (v/v) FBS along with CHIR 99021 (2 μM) and FGF4 (500 ng/mL). After 3–4 days, free-floating epithelial spheres and loosely attached epithelial tubes were harvested. Epithelial structures were subsequently suspended in Matrigel and overlaid in intestinal organoid medium containing CHIR99021 (2 μM), noggin and EGF (both 100 ng/mL), and B27 (1×). Organoids were sorted for EPCAM, an epithelial cell marker, 30 days after differentiation and passaged every 7–10 days thereafter.

GHR knockout mice

GHR$^{-/-}$ mice (B6N[Cg]-Ghrtm1b[KOMP]wtsi/3J) were purchased from The Jackson Laboratory. Breeding was performed with heterozygous males and females, so WT and *GHR*$^{-/-}$ mice were obtained from the same breeding. Heterozygous mice were backcrossed with WT at least 5 times, and 3- and 24-month old male mice were included in the study.

Xenograft model

HCT116 cells transduced with lentivirus-expressing murine GH (Lenti-mGH) or empty vector (Lenti-V) (5×10^5 cells in 0.05 mL PBS) were mixed (1:1) with High Concentration Matrigel Matrix and injected subcutaneously into the right flank of 8-week old athymic nude mice (The Jackson Laboratory) to establish an *in vivo* model of excess systemic GH. Control mice were injected with HCT116 cells transduced with an empty vector. All mice developed xenograft tumors and were sacrificed 5 weeks after injection. The middle part of colons were harvested from each mouse, washed with cold PBS, snap freezed and homogenized, lysed in RIPA buffer with protease inhibitors. Circulating levels of GH in Lenti-mGH mice were measured by murine GH ELISA.[17]

Human blood samples

Diagnosis of acromegaly was made based on symptoms and signs, evidence of a pituitary adenoma on magnetic resonance imaging, and elevated serum concentrations of IGF1 (>1.3 × upper limit of normal). Non-functioning adenomas were diagnosed in the absence of clinical and biochemical evidence of pituitary adenoma-related hormone hypersecretion in subjects with a pituitary adenoma on magnetic resonance imaging.[79]

On the day of surgery, blood samples were collected, and buffy coats freshly separated from the peripheral blood of enrolled subjects using Histopaque 1077 solution.

Constructs and transfections

Lentiviral particles expressing human GH shRNA, Src shRNA or nontargeted control shRNA (GFP Control Lentiviral Particles) are from Santa Cruz Biotechnology.

Lentiviral particles expressing hGH (pLV-EF1p-hGH1-IRES-eGFP-WPRE), respective control lentiviral particles (pLV-EF1p-mCherry-IRES-eGFP-WPRE), murine GH (EF1-luc2-GH-Ubic), and respective control vector (EF1-luc2-Ubic) were generated at the Regenerative Medicine Institute at Cedars-Sinai.

hNCC or HCT116 were plated 1 day before transfections and were transduced with 50 MOI lentivirus particles with 8 μg/mL polybrene. Cells were cultured overnight, medium was changed, and cells were split 48 h later then used for experiments 10 days after transduction.

Organoids were dispersed into single-cell suspension using TrypLE and mixed with Matrigel together with 50 MOI lentiviral particles and 8 μg/mL polybrene. Cells in the Matrigel bubble were plated into 24-well plates and overlaid with intestinal organoid media enriched with 10 nM Rock inhibitor, 500 nM A8301, and 10 μM SB202190.

METHOD DETAILS

Treatments

Human recombinant GH was purchased from BioVision and reconstituted in PBS pH 8 containing 0.1% BSA. Previously, we have shown that, different doses of GH (50–500 ng/mL) had similar effects[17]; here, cells were treated with 500 ng/mL GH, a well-accepted dose for *in vitro* experiments.[80–84]

The GH antagonist pegvisomant[85] was provided by Pfizer. Etoposide, WIP1 inhibitor (GSK2830371), AMPK inhibitor (Compound C, CAS 866405-64-3) and Src inhibitor (dasatinib, BMS-354825) were reconstituted in DMSO at a stock concentration of 50 mM. The GHR synthesis inhibitor antibody BM001[52] was provided by Specs (Zoetermeer, The Netherlands) and reconstituted in DMSO at a stock concentration of 10 mM.

For BM001 injections, 3-month-old WT female mice were purchased from The Jackson Laboratory.

Protein analysis

Cells were homogenized and lysed in RIPA buffer with protease. Proteins were separated by SDS-PAGE, electroblotted onto Trans-Blot Turbo Transfer Pack 0.45 μm PVDF membrane, and incubated overnight with indicated primary antibodies, followed by corresponding horseradish peroxidase–conjugated secondary antibodies: anti-goat, anti-mouse, or anti-rabbit. Hikari signal enhancer kit was used to detect low abundance proteins. Immunoblot signals were amplified using BIO-RAD Molecular Imager ChemiDoc XRS+ System. For information about antibodies, see key resources table.

Cytoplasmic and nuclear protein separation was performed using NE-PER Nuclear and cytoplasmic Extraction Reagents according to the manufacturer's protocol.

Immunoprecipitation

hNCC were plated in 10 cm dishes in full PriGrow III media and treated the next day with 20 μM of etoposide for 24 h. Cells were then washed and media changed for serum-free media (with 0.1% BSA) with GH or no GH for another 24 h. hNCC were collected in immunoprecipitation buffer with protease inhibitors and phosphatase inhibitors. After proteins were isolated, concentrations were measured using the DC method and 2 mg protein used per reaction. IP was performed according to the manual, and 5 μg of mouse IgG as control, 5 μg of anti-ubiquitin, 5 μg anti-HIPK2 antibodies, or 5 μg anti-WIP1 antibody were used per immunoprecipitation reaction. Denatured proteins dissociated from beads were analyzed by SDS/PAGE.

Immunocytochemistry

hNCC line #1 cells were plated on coverslips pretreated with ECL Cell Attachment Matrix; the next day, media was changed for serum-free with GH for 24 h then cells were fixed with 4% PFA/PBS for 20 min. Cells were permeabilized with 0.25% Triton X-100 for 30 min and blocked in 10% donkey serum in 1% BSA/PBS. Anti-WIP1 mouse primary antibodies and anti-HIPK2 rabbit antibodies diluted in 10% donkey serum were added overnight, followed by secondary donkey anti-mouse Alexa Fluor 488, anti-rabbit Alexa Fluor 568 antibodies, and Alexa Fluor 647 phalloidin in 1% BSA/PBS for 1 h. Samples were imaged with a Stellaris confocal microscope (Leica Microsystems).

Comet assay

The extent of DNA damage in individual cells was measured by using an OxiSelect Comet Assay kit according to the manufacturer's instructions. Single-cell alkaline electrophoresis was performed for 30 min at 1 V/cm. DNA damage was quantified by ImageJ as the percent of damaged DNA in the tail to the entire cell DNA (intensity of the staining) multiplied by the length of the tail (Olive tail moment = tail DNA% × tail moment length). Data collected from at least 3 independent experiments and at least 400 nuclei/group were analyzed.

Real-time PCR

Total RNA was isolated with TRIzol followed by RNAeasy mini Kit. After DNAse I treatment (TURBO DNA free), cDNA was synthesized from 1 μg purified RNA by the SuperScript II First-Strand cDNA synthesis system. Quantitative PCR was performed in 20 μL reactions using SsAdvanced SYBR Green Supermix in BioRad CFX 96 Touch Real-Time PCR System. For primers, see key resources table. Reactions were performed in triplicate. Relative mRNA quantities in experimental samples were determined by CFX Maestro 1.0 software, expressed in arbitrary units as fold-difference from control.

Nucleofection

hNCC line#1 were trypsinized, washed, and 1×10^6 cells were placed into 100 μL of Nucleofector Solution with 30 pmol/sample of control human siRNA or WIP1 siRNA and nucleofected using W-001 program of Amaxa Nucleofector I. Each nucleofected sample was plated into 2 wells of 6-well plate in 2 mL of full Prigrow III media overnight; media was then changed to serum free media containing 0.1% BSA with or without 500 ng/mL GH for an additional 6 h.

QUANTIFICATION AND STATISTICAL ANALYSIS

Data are presented as mean ± SEM. Differences between treatment group means were tested with ANOVA and included the factor of experimental replicate where appropriate (up to 4 replicates performed). Data from acromegaly and NFA patients were analyzed with mixed model regression to control for repeated testing of subject data across experimental replicates with sex included as a fixed effect. Post-hoc pairwise comparisons were Tukey-adjusted for multiple testing. Residuals were checked to confirm assumptions were met for parametric assessment, and, when necessary, the non-parametric Kruskal-Wallis test followed by Dunn's multiple comparison test was used. Differences were considered significant where $p < 0.05$. Analysis was performed with SAS v9.4 and GraphPad Prism9 software.